Exploring the impacts of unprecedented climate extremes on forest ecosystems: hypotheses to guide modeling and experimental studies

Jennifer A. Holm[1,*], David M. Medvigy[2], Benjamin Smith[3,4], Jeffrey S. Dukes[5], Claus Beier[6],

Mikhail Mishurov[3], Xiangtao Xu[7], Jeremy W. Lichstein[8], Craig D. Allen[9], Klaus S. Larsen[6], Yiqi

Luo[10], Cari Ficken[11], William T. Pockman[12], William R.L. Anderegg[13], and Anja Rammig[14]

[1] Lawrence Berkeley National Laboratory, Berkeley, California, USA

[2] University of Notre Dame, Notre Dame, Indiana, USA
[3] Dept of Physical Geography and Ecosystem Science, Lund University, Lund, Sweden
[4] Hawkesbury Institute for the Environment, Western Sydney University, Penrith, NSW 2751, Australia
[5] Department of Forestry and Natural Resources and Biological Sciences, Purdue University, West Lafayette, Indiana, USA
[6] Department of Geosciences and Natural Resource Management, University of Copenhagen, Frederiksberg, Denmark
[7] Department of Ecology and Evolutionary Biology, Cornell University, Ithaca, New York, USA
[8] Department of Biology, University of Florida, Gainesville, Florida, USA
[9] U.S. Geological Survey, Fort Collins Science Center, New Mexico Landscapes Field Station, Los Alamos, New Mexico, USA
[10] Center for Ecosystem Science and Society, Department of Biological Sciences, Northern Arizona University, Flagstaff, Arizona, USA
[11] Department of Biology, University of Waterloo, Waterloo, Ontario, Canada
[12] Department of Biology, University of New Mexico, Albuquerque, New Mexico, USA
[13] School of Biological Sciences, University of Utah, Salt Lake City, Utah, USA
[14] Technical University of Munich, TUM School of Life Sciences Weihenstephan, Freising, Germany

* *Correspondence to*: Jennifer Holm; 510-495-8083; jaholm@lbl.gov

34 **Abstract**

35

36 Climatic extreme events are expected to occur more frequently in the future, increasing the

37 likelihood of unprecedented climate extremes (UCEs), or record-breaking events. UCEs, such as

38 extreme heatwaves and droughts, substantially affect ecosystem stability and carbon cycling by

39 increasing plant mortality and delaying ecosystem recovery. Quantitative knowledge of such

40 effects is limited due to the paucity of experiments focusing on extreme climatic events beyond

41 the range of historical experience. Here, we present a road map of how two dynamic vegetation

42 demographic models (VDMs) can be used to investigate hypotheses surrounding ecosystem

43 responses to UCEs (e.g., unprecedented droughts). As a result of nonlinear ecosystem responses

44 to UCEs, that are qualitatively different from responses to milder extremes, we consider both

45 biomass loss and recovery rates over time, by reporting a time-integrated carbon loss as a result

46 of UCE, relative to the absence of drought. Additionally, we explore how unprecedented

47 droughts in combination with increasing atmospheric CO_2 and/or temperature may affect

48 ecosystem stability and carbon cycling. We explored these questions using simulations of pre-

49 drought and post-drought conditions at well-studied forest sites, using the ED2 and LPJ-GUESS

50 models. Due to the two models having different but plausible representations of processes and

51 interactions, they diverge in sensitivity of nonlinear biomass loss due to drought duration or

52 intensity, and differ between each site. Biomass losses are most sensitive to drought duration in

53 ED2, but to drought intensity in LPJ-GUESS. Elevated atmospheric CO_2 concentrations (eCO_2)

54 alone did not completely buffer the ecosystems from carbon losses during UCEs in the majority

55 of our simulations. Our findings highlight contrasting differences in process formulations and

56 uncertainties in models, most notably related to availability in plant carbohydrate storage and the

57 diversity of plant hydraulic schemes, in projecting potential ecosystem responses to UCEs. We

58 provide a summary of the current state and role of many model processes that give way to

59 different underlying hypotheses of plant responses to UCEs, reflecting knowledge gaps, which

60 should be tested with targeted field experiments and an iterative modeling-experimental

61 conceptual framework.

Deleted: As an example, we investigate whether ecosystem responses to UCEs are qualitatively different from responses to milder extremes, as a result of non-linear ecosystem responses. …

Deleted: in Australia and Costa Rica

Deleted: Both models produced nonlinear responses to UCEs. …

Deleted: Our model review uncovered

2

1 Introduction

The increase in extreme climate and weather events, such as prolonged heatwaves and droughts as seen over the last three decades, are expected to continue to increase in frequency and magnitude, leading to progressively longer and warmer droughts on land (IPCC 2012, 2021). Droughts are affecting all areas of the globe, more than any other natural disturbance, and recent droughts have broken long-standing records (Ciais et al., 2005; Phillips et al., 2009; Williams et al., 2012; Matusick et al., 2013; Griffin and Anchukaitis, 2014; Asner et al., 2016; Feldpausch et al., 2016; Seneviratne et al., 2021). Such 'unprecedented climate extremes' (UCEs; "record-breaking events", IPCC (2012)) that are larger in extent and longer-lasting than historical norms can have dramatic consequences for terrestrial ecosystem processes, including carbon uptake and storage and other ecosystem services (Reichstein et al., 2013; Settele, 2014; Allen et al., 2015; Brando et al., 2019; Kannenberg et al., 2020). Thus, to better anticipate the implications of climatic changes for the terrestrial carbon sink and other ecosystem services, we need to better understand how ecosystems respond to extreme droughts and other UCEs.

To learn how ecosystems respond to rarely experienced or unprecedented conditions, ecologists can experimentally manipulate environmental conditions (Rustad, 2008; Beier et al., 2012; Meir et al., 2015; Aguirre et al., 2021). However, the majority of such experiments apply moderate treatments based on a historical sense, which are mostly weaker in intensity and/or shorter in duration than potential future UCEs (Beier et al., 2012; Kayler et al., 2015; but see Luo et al., 2017), and single experiments have low power to detect effects of stressors on ecosystem responses (Yang et al., 2022). Additionally, most experiments examine low-stature ecosystems, such as grassland, shrubland or tundra, due to lower requirements for infrastructure and financial investment compared to mature forests. However, forests may respond qualitatively differently to UCEs than other ecosystems, in part due to mortality of large trees and strong nonlinear ecosystem responses, with long-lasting consequences for ecosystem-climate feedbacks (Williams et al., 2014; Meir et al., 2015). Ecosystem responses to naturally occurring extreme droughts and heatwaves have been documented (Ciais et al., 2005; Breshears et al., 2009; Feldpausch et al., 2016; Matusick et al., 2016; Ruthrof et al., 2018; Powers et al,. 2020); however, these rapidly-mobilized post-hoc studies often are unable to measure all critical variables and may lack consistently collected data for comparison with pre-drought conditions, thus limiting their inferential power and ability to improve quantitative models. The difficulties of performing

3

101   controlled real-world experiments of UCEs at broad spatial and temporal scales make process-

102   based modeling a valuable tool for studying potential ecosystem responses to extreme events.

103   Process-based models can be used to explore potential ecosystem impacts using projected

104   climate change over broad spatial and temporal scales (Gerten et al., 2008; Luo et al., 2008;

105   Zscheischler et al., 2014; Sippel et al., 2016), as seen in a few modeling studies that have

106   synthesized and improved our process-level understanding of UCE effects (McDowell et al.,

107   2013; Dietze and Matthes, 2014). However, due to the overly simplified representation of

108   ecological processes in most land surface models (LSMs) – the terrestrial components of Earth

109   System Models (ESMs) used for climate projections – it is doubtful whether most of these

110   models adequately capture ecosystem feedbacks and other responses to UCEs (Fisher and

111   Koven, 2020). For example, only a few ESMs in recent coupled model intercomparison projects

112   (CMIP6) and IPCC climate assessments (Ciais et al., 2013; Arora et al., 2020) include vegetation

113   demographics (Döscher et al., 2022), and most rely on prescribed, static maps of plant functional

114   types (PFTs) (Ahlström et al., 2012). Other LSMs simulate PFT shifts (i.e., dynamic global

115   vegetation models, DGVMs; Sitch et al., (2008)) based on bioclimatic limits, instead of

116   emerging from the physiology- and competition-based demographic rates that determine

117   resource competition and plant distributions in real ecosystems (Fisher et al., 2018). Although a

118   new generation of LSMs with more explicit ecological dynamics and structured demography is

119   emerging (Holm et al., 2020; Koven et al., 2020; Döscher et al., 2022), most current ESMs are

120   limited in ecological detail and realism (e.g., ecosystem structure, demography, and

121   disturbances). Failing to mechanistically represent mortality, recruitment, and disturbance – each

122   of which influences biomass turnover and carbon (C) allocation (Friend et al., 2014) – limits the

123   ability of these models to realistically forecast ecosystem responses to anomalous environmental

124   conditions like UCEs (Fisher et al., 2018).

125   Evaluating and improving the representation of physiological and ecological processes in

126   ecosystem models is critical for reducing model uncertainties when projecting the effects of

127   UCEs on long-term ecosystem dynamics and functioning. Vegetation demography, plant

128   hydraulics, enhanced representations of plant trait variation, explicit treatments of resource

129   competition (e.g., height-structured competition for light), and representing major disturbances

130   (e.g., extreme drought) have all been identified as critical areas for advancing current models

131   (Scheiter et al., 2013; Fisher et al., 2015; Weng et al., 2015; Choat et al., 2018; Fisher et al.,

Deleted: (Table 1)

133 2018; Blyth et al., 2021) and are necessary advances for realistically representing the ecosystem
134 impacts of UCEs. In this perspectives focused paper we look at the differences in these
135 processes, and how they contribute to uncertainty across multiple temporal phases surrounding
136 an extreme event: predicting an ecosystem's pre-disturbance resistance, which influences the
137 degree of impact and recovery from UCEs. Table 1 describes a summary of model mechanisms
138 that affect pre-drought resistance and post-drought recovery and we suggest are critical areas
139 further research (ca. Frank et al., 2015).
140   In order to inform our discussion, we explore the potential responses of forest ecosystems
141 to UCEs using two state-of-the-art process-based demographic models (vegetation demographic
142 models, VDMs; Fisher et al., (2018)), a unique model exploration-discussion approach to help
143 highlight new paths forward for model advancement. We first present conceptual frameworks
144 and hypotheses on potential ecosystem responses to UCEs based on current knowledge. We then
145 present VDM simulations for a range of hypothetical UCE scenarios to illustrate current state-of-
146 the-art model representations of eco-physiological mechanisms expected to drive responses to
147 UCEs. While a variety of UCE-linked biophysical tree disturbance processes (e.g., fire, wind,
148 insect outbreaks) can drive nonlinear ecosystem responses, we focus specifically on extreme
149 droughts, which have important impacts on many ecosystems around the world (e.g. Frank et al.,
150 2015, IPCC 2021). By studying modeled responses to UCEs, we explore the limits to our current
151 understanding of ecosystem responses to extreme droughts and their corresponding thresholds
152 and tipping points. As anthropogenic forcing has increased the frequency, duration, and intensity
153 of droughts throughout the world (Chiang et al., 2021), we explore how eCO_2 and rising
154 temperatures may affect drought-induced C loss and recovery trajectories, and how the scientific
155 community can iteratively address these questions through experiments and modeling studies.
156 We believe the combination of using cutting-edge VDMs alongside an inspection of current gaps
157 in knowledge will help guide modeling and experimental advances in order to address novel
158 forest responses to climate extremes.
159
160 **1.1 Conceptual and Modeling Framework for Hypothesis Testing:**
161   We combine conceptual frameworks (Fig. 1) and ecosystem modeling to test two
162 hypotheses on potential responses of plant carbon stocks to UCEs. The first hypothesis is:

Deleted: drought

Deleted: (

Deleted:)

Deleted: -

Deleted: review

168 *Hypothesis (H1). Terrestrial ecosystem responses to UCEs will differ qualitatively from*
169 *ecosystem responses to milder extremes because responses are nonlinear. Nonlinearities can*
170 *arise from multiple mechanisms – including shifts in plant hydraulics, C allocation,*
171 *phenology, and stand demography – and can vary depending on the pre-drought state of the*
172 *ecosystem.*

173 We present four conceptual relationships that describe terrestrial ecosystem responses to varying
174 degrees of extreme events (Fig. 1). Change in vegetation C stock is related to drought intensity
175 and/or drought duration in a near-linear relationship (Fig. 1a, H0, null hypothesis), which has
176 some observational support from annual and perennial grassland ecosystems, shrublands and
177 savannas across the globe (Bai et al., 2008; Muldavin et al., 2008; Ruppert et al., 2015). We
178 recognize that most ecological systems are nonlinear, thus alternatives to the null hypothesis are
179 that biomass loss increases nonlinearly with increased drought intensity (i.e., reduction in
180 precipitation) represented by a threshold-based relationship (Fig. 1a, H1a), increased drought
181 duration (i.e., prolonged drought with the same intensity) by shifting the near-linear relationship
182 downwards via increasing slopes (Fig. 1a, H1b), or the combination of both intensity and
183 duration (Fig. 1a, H1c). These hypotheses are supported by observations from the Amazon Basin
184 and Borneo (Phillips et al., 2010) where tree mortality rates increased nonlinearly with drought
185 intensity. Similarly, plant hydraulic theories predict nonlinear damage to the plant-water
186 transport systems, and thus mortality risk, as a function of drought stress (Sperry and Love,
187 2015). In particular, longer droughts are more likely to lead to lower soil water potentials,
188 leading to a nonlinear xylem damage function even if stomata effectively limit water loss (Sperry
189 et al., 2016).

190 *Hypothesis (H2): The effects of increasing atmospheric CO_2 concentration (eCO2) will*
191 *alleviate impacts of extreme drought stress through an increase in vegetation productivity and*
192 *water-use efficiency, but only up to a threshold of drought severity, while increased*
193 *temperature (and related water stress) will exacerbate tree mortality.*
194 This second hypothesis is based on growing evidence that effects of eCO2 and climate
195 warming may interact with effects of drought intensity on ecosystems. The CO_2 fertilization
196 effect enhances vegetation productivity (e.g., net primary production, NPP) (Ainsworth and
197 Long, 2005; Norby et al., 2005; Wang et al., 2012), but this fertilization effect is generally

Deleted: *linearly*

Deleted: A

Deleted: (linear)

Deleted: -

Deleted: -

6

203 reduced by drought (Hovenden et al., 2014; Reich et al., 2014; Gray et al., 2016). Drought events

204 often coincide with increased temperature, which intensifies the impact of drought on

205 ecosystems (Allen et al., 2015; Liu et al., 2017), resulting in nonlinear responses in mortality

206 rates (Adams et al., 2009; Adams et al., 2017a). The evaluation of C cycling in VDMs with

207 doubling of CO_2 (only "beta effect") showed a large carbon sink in a tropical forest (Holm et al.,

208 2020), but the inclusion of climate interactions in VDMs needs to be further explored.

209   Here, we relate ecosystem responses to UCEs by calculating the "integrated carbon (C)

210 loss" (Fig. 1b and see Methods), which integrates C loss from the beginning of the drought until

211 the time when C stocks have recovered to 50% of the pre-drought level. In response to drought,

212 warming, and eCO_2, divergent potential C responses (gains and losses; Fig. 1c) can be expected

213 (Keenan et al., 2013; Zhu et al., 2016; Adams et al., 2017a). For example, a grassland

214 macrocosm experiment found that eCO_2 completely compensated for the negative impact of

215 extreme drought on net carbon uptake due to increased root growth and plant nitrogen uptake,

216 and led to enhanced post-drought recovery (Roy et al., 2016). However, a 16-year grassland

217 FACE and the SoyFACE experiments showed that CO_2 fertilization effects were reduced or

218 eliminated under hotter/drier conditions (Gray et al., 2016; Obermeier et al., 2016). Reich et al.,

219 (2014) also found that CO_2 fertilization effects were reduced in a perennial grassland by water

220 and nitrogen limitation.

221   A corollary to our H2 is that conditions that favor productivity (e.g., longer growing

222 seasons and/or CO_2 fertilization) will enhance vegetation growth leading to "structural

223 overshoot" (SO; Fig. 1d; adapted from and supported by Jump et al., 2017), and can amplify the

224 effects of UCEs. Enhanced vegetation growth coupled with environmental variability can lead to

225 exceptionally high plant-water-demand during extreme drought and water stress, resulting in a

226 "mortality overshoot" (MO; Fig 1d). We conceptualize how oscillations between SO and

227 associated MO could be amplified by increasing climatic variability and UCEs (Fig. 1d).

228 Confidence is low as to how historically unprecedented eCO_2 levels and temperatures will affect

229 ecosystems in the future (i.e., the widening of the shaded areas compared to historical, Fig. 1d).

230 We expect, however that a rapidly changing climate, combined with effects of UCEs as a result

231 of more frequent extreme drought/heat events and drought stress, can exacerbate and amplify

232 SOs and MOs (Jump et al., 2017), leading to increasing C loss, even though various buffering

7

233 mechanisms exist (cf. (Lloret et al., 2012; Allen et al., 2015)). Relative to our conceptual (Fig.

234 1d), we note that most experimental, observational and modeling studies (Ciais et al., 2005; da

235 Costa et al., 2010; Phillips et al., 2010; Meir et al., 2015) take into account only low to moderate

236 drought intensities (such as 50% rain excluded) or single events, or combine drought with

237 moderate effects of temperature change. Where there has been 100% rain exclusion, it was on

238 very small plots of 1.5 m^2 (Meir et al., 2015). As represented by the increasing amplitude of

239 oscillations in Fig. 1d, the interactions between increased temperatures, UCE events, and

240 vegetation feedbacks make ecosystem states become inherently unpredictable, particularly over

241 longer time-scales.

242

243 **2 Vegetation Demography Model (VDM) Approaches**

244   We argue that VDMs are well suited to address climate change impacts due to the

245 inclusion of detailed process representation of dynamic plant growth, recruitment, and mortality,

246 resulting in changes in abundance of different PFTs, as well as vertically stratified tree size- and

247 age-class structured ecosystem demography. Community dynamics and age-/size-structure are

248 emergent properties from competition for light, space, water, and nutrients, which dynamically

249 and explicitly scale up from the tree, to stand, to ecosystem level. Within this characterization,

250 VDMs also differ between each other and are set up in different configuration, allowing for

251 various testing capabilities. For full names of each model listed below and references, see Table

252 S1. For example, VDMs can aggregate and track the community level disturbance into either

253 patch-tiling sampling (e.g., ED2, FATES, LM3-PPA, ORCHIDEE, JSBACH4.0) or statistical

254 approximations (e.g., LPJ-GUESS, SEIB-DGVM, and CABLE-POP). VDMs could also vary in

255 representing light competition within either multiple canopy layers (e.g., ED2, FATES, LM3-

256 PPA, LPJ-GUESS, SEIB-DGVM) or in a single canopy (e.g., JSBACH4.0, ORCHIDEE,

257 CABLE-POP).

258   Powell et al. (2013) compared multiple VDMs and LSMs to interpret ecosystem

259 responses to long-term droughts in the Amazon and are informative when conducting model-data

260 comparisons, but studies of the cascade of ecosystem responses and mortality to UCEs are

261 lacking. In a cutting-edge area of development, new mechanistic implementation of plant

262 competition for water and plant hydraulics in VDMs (i.e., hydrodynamics) are improving our

263 understanding of plant-water relations and stresses within plants, such as with TFSv.1-Hydro

8

(Christoffersen et al., 2016), ED2-hydro (Xu et al., 2016), and FATES-HYDRO (Ma et al., 2021; Fang et al., 2022). Compared to more simplistic representation of plant acquiring soil moisture not connected to plant physiology (e.g., LPJ-GUESS, LM3-PPA, CABLE-POP, SEIB-DGVM). For hydrodynamic representations in 'big-leaf' LSMs such as CLM5, JULES, and Noah-MP-PHS see Kennedy et al., (2019), Eller et al., (2020), and Li et al., (2021) respectively.

The discussion section provides a deeper investigation of model response to UCEs related to droughts. An exhaustive review of all VDMs, and all plant processes is too large to be done here. Existing review papers of different VDM development, processes, and uncertainties can be found here: Fisher et al., (2018); Bonan (2019); Trugman et al., (2019); Hanbury-Brown et al. (2022); Bugmann and Seidl (2022); and specifically related to plant hydraulics see: Mencuccini et al., (2019); Anderegg and Venturas (2020). We use LPJ-GUESS and ED2 as example VDMs in an initial guide framework to explore hypotheses around vegetation mortality and integrated carbon loss from UCEs and climate change impacts, and highlight limiting model processes. Since field data needed to evaluate UCE responses are, by definition, unavailable, we do not perform model-data comparisons. Rather, we use the model results and conceptual framework as a road map to explore our hypotheses and illustrate their implications for ecosystem responses under UCEs, not historical drought events.

2.1 LPJ-GUESS and ED2 Model Descriptions

We explored our hypotheses at forested ecosystems in Australia and Central America using two VDMs: the Lund-Potsdam-Jena General Ecosystem Simulator (LPJ-GUESS) (Smith et al., 2001; Smith et al., 2014) and the Ecosystem Demography model 2 (ED2) (Medvigy et al., 2009; Medvigy and Moorcroft, 2012). Both LPJ-GUESS and ED2 resolve vegetation into tree cohorts characterized by their PFT, in addition to age-class in LPJ-GUESS; and size, and stem number density in ED2. Both models are driven by external environmental drivers (e.g., temperature, precipitation, solar radiation, atmospheric CO_2 concentration, nitrogen deposition), and soil properties (soil texture, depth, etc.), and also depend on dynamic ecosystem state, which includes light attenuation, soil moisture, and soil nutrient availability. Establishment and growth of PFTs, and their carbon-, nitrogen- and water-cycles, are simulated across multiple patches per grid cell to account for landscape heterogeneity. Both models characterize PFTs by physiological

322   and bioclimatic parameters, which vary between the models (Smith et al., 2001; Smith et al.,

323   2014; Medvigy et al., 2009; Medvigy and Moorcroft, 2012).

324   The LPJ-GUESS includes three woody PFTs: evergreen, intermediate evergreen, and

325   deciduous PFTs. Mortality in LPJ-GUESS is governed by a 'growth-efficiency'-based function

326   (kg C m^{-2} leaf yr^{-1}), which captures effects of water deficit, shading, heat stress, and tree size on

327   plant productivity relative to its resource-uptake capacity (leaf area), with a threshold below

328   which stress-related mortality risk increases markedly, in addition to background senescence and

329   exogenous disturbances. Stress mortality can be reduced by plants using labile carbon storage,

330   modeled implicitly using a 'C debt' approach, which buffers low productivity, enhancing

331   resilience to milder extremes (more details are given in section 4.1.4). Total mortality can thus be

332   impacted by variation in environmental conditions such as water limitation, low light conditions,

333   and nutrient constraints, as well as current stand structure (Smith et al., 2001; Hickler et al.,

334   2004).

335   The ED2 version used here (Xu et al., 2016) includes four woody PFTs: evergreen,

336   intermediate evergreen, deciduous, brevi-deciduous, and deciduous stem-succulent. This ED2

337   version includes coupled photosynthesis, plant hydraulics, and soil hydraulic modules (Xu et al.,

338   2016), which together determine plant water stress. The plant hydraulics module tracks water

339   flow along a soil–plant–atmosphere continuum, connecting leaf water potential, stem sap flow,

340   and transpiration, thus influencing controls on photosynthetic capacity, stomatal closure,

341   phenology, and mortality. Leaf water potential depends on time-varying environmental

342   conditions as well as time-invariant PFT traits. Leaf shedding is triggered when leaf water

343   potential falls below the turgor loss point (a PFT trait) for a sufficient amount of time. Leaf

344   flushing occurs when stem water potential remains high (above half of the turgor loss point) for a

345   sufficient time (see Xu et al., 2016 for details). PFTs differ in their hydraulic traits, wood

346   density, specific leaf area, allometries, rooting depth, and other traits. Stress-based mortality in

347   the ED2 version used here includes two main physiological pathways in our current

348   understanding of drought mortality (McDowell et al., 2013): C starvation and hydraulic failure.

349   Mortality due to C starvation in ED2 results from a reduction of C storage, a proxy for non-

350   structural carbohydrate (NSC) storage, which integrates the balance of photosynthetic gain and

351   maintenance cost under different levels of light and moisture availability. Mortality due to

10

352   hydraulic failure in ED2 is based on the percentage loss of stem conductivity. ED2 also includes

353   a density-independent senescence mortality rate based on wood density.

2.2 Modeling guide

355   To exemplify how VDMs can be tools to explore new hypotheses related to UCEs we

356   applied the models at two field sites, that were chosen due to being extensively studied and the

357   models used here have already been run at these sites and previously benchmarked against field

358   data (see Xu et al., 2016; Medlyn et al., 2016; Medvigy et al., 2019 for model-data validation).

359   The purpose of this paper was not to do a large multi-site comparison, but rather just select a few

360   for hypothesis testing. In addition, the two sites span a range of vegetation types and are in

361   warm, seasonally dry climates that are more likely to experience droughts in the future (Allen et

362   al., 2017). The first is a mature *Eucalyptus* (*E. tereticornis*) warm temperate-subtropical

363   transitional forest that is the site of the Eucalyptus Free Air CO_2 enrichment (EucFACE)

364   experiment in Western Sydney, Australia (Medlyn et al., 2016; Ellsworth et al., 2017; Jiang et

365   al., 2020). The second site is a seasonally dry tropical forest in the Parque Nacional Palo Verde

366   in Costa Rica (Powers et al., 2009). Site description details can be found in Supplement Text A.

367   We performed a 100-year "baseline" simulation for each model at each site driven by

368   constant, near ambient, atmospheric CO_2 (400 ppm) and recycled historical site-specific climate

369   data (1992-2011 for EucFACE and 1970-2012 for Palo Verde; Sheffield et al., (2006)), absent of

370   drought treatments. A detailed description of the meteorological data and initial conditions used

371   to drive the models is in the Supplementary Text A. The two models were previously tuned for

372   each site (Xu et al., 2016; Medlyn et al., 2016), and no additional site-level parameter tuning was

373   conducted here due to evaluating responses from hypothetical UCEs. To describe the ecosystem

374   impact of UCEs, we simulated 10 years of pre-drought conditions (continuing from the baseline

375   simulation), followed by drought treatments that differed in intensity and duration, followed by a

376   100-year post-drought recovery period. To explore the effects of drought intensity, we conducted

377   20 different artificial drought intensity simulations, in which precipitation during the whole year

378   is reduced by 5% to 100% of its original amount, in increments of 5%. To explore the effects of

379   drought duration, the 20 different drought intensities are maintained over 1, 2 and 4 years (Table

380   S2). We examined model responses of aboveground biomass, leaf area index (LAI), stem density

381   (number ha^{-1}), plant available soil water (mm), plant C storage (kg C m^{-2}), change in stem

382   mortality rate (yr^{-1}), and PFT composition.

402   To explore how temperature, eCO$_2$ concentration, and UCE droughts influence forest C
403   dynamics individually and in combination, we implemented the following five experimental
404   scenarios, some realistic and others hypothetical, for each model (Table S2): increased

405   temperature only (+2K over ambient), eCO$_2$ only (600 ppm and 800 ppm), and both increased
406   temperature and eCO$_2$ (+2K 600 ppm; +2K 800 ppm). Temperature and eCO$_2$ manipulations
407   were applied as step increases over the baseline conditions, and are artificial scenarios, as
408   opposed to model-generated climate projections.
409
410   **2.3 Linking concepts, hypotheses, and model outcomes**
411   To relate our simulation results to Fig. 1a, we compared the total biomass loss as a result
412   of each drought treatment by calculating the percentage of biomass reduction at the end of the
413   drought period relative to the baseline (no drought) simulation. To explicitly consider biomass
414   recovery rates over time, we calculated "integrated-C-loss" (Eqs. 1-3), as a result of drought
415   under current climate, which are determined based on the concepts in Fig. 1b. We defined
416   "integrated-C-loss" as the time-integrated carbon in biomass that is lost due to drought relative to
417   what the vegetation would have stored in the absence of drought. That is, it is the difference
418   between biomass in the presence of drought (B$_d$) at time (t) and biomass in the baseline
419   simulation (no drought; B$_{base}$), integrated over a defined recovery time period (in kg C m^{-2}
420   yr):

$$\text{Integrated-C-loss} = \int_{t=t_1}^{t=t_2} (B_{base}(t) - B_d(t))\, dt$$

421   (Eq. 1)

422   To define the bounds of integration, in Eq. 1, t_1 is defined as the time when the maximum
423   amount of plant C is lost as a result of the drought:

$$B_{base}(t_1) - B_d(t_1) = \max_t [B_{base}(t) - B_d(t)]$$

424   (Eq. 2)

425   Then, t_2 is defined implicitly as the time when 50% of the lost biomass has been recovered
426   compared to the baseline:

$$B_{base}(t_2) - B_d(t_2) = \frac{1}{2}(B_{base}(t_1) - B_d(t_1))$$

427   (Eq. 3)

12

429   Since all integrated-C-loss results are taken as the difference from a non-drought baseline

430   biomass (B_{base}) and all droughts will result in a loss of C.

431   We also use integrated-C-loss to examine the role of drought, temperature and eCO_2

432   change for moderating or exacerbating the impacts of drought on forest C stocks; i.e., to evaluate

433   the hypotheses illustrated in Fig. 1c. To assess these impacts of changing climates, we calculate

434   an "integrated-C-change" (Eq. 4). Defined as the difference between the integrated-C-loss due to

435   drought alone (Eqs. 1-3) under present climate, and the integrated-C-loss due to the combined

436   effects of drought and climate change (i.e., five scenarios of temperature increase and eCO_2):

$$\text{Integrated-C-change} = integrated\ C\ Loss_{Drought} - integrated\ C\ Loss_{Drought+CC}$$

437   (Eq. 4)

438   Because we expect drought to reduce vegetation C stocks, and thus integrated-C-loss to

439   be negative, positive values of integrated-C-change indicate that changes in climatic drivers

440   reduced the C losses from drought (i.e., buffering effects). Negative values of integrated-C-

441   change indicate that the climate change scenario leads to either greater C losses or losses that

442   persist for longer amounts of time (i.e., magnitude and/or duration) compared to a simulation

443   with no climate change (i.e., "reference" run).

444

445   **3 Results**

446   As a basis for the treatment results presented here, we compared the baseline simulations

447   (prior to drought or climate change treatments) of the two VDMs to observations at both sites for

448   biomass and LAI (Table S3, Fig. S1). Both models had similar biomass compared to   Deleted: 2

449   observations at Palo Verde (10.4 - 11.7 vs. 11.0 kgC m^{-2}), and at EucFACE biomass matched

450   well in LPJ-GUESS (12.1 vs. 12.7 kgC m^{-2}) but was low in ED2 (5.6 kgC m^{-2}). Both models also

451   had similar LAI to observations at Palo Verde (3.3 – 4.5 vs. 3.8 ($\pm$ 1.06) m^2 m^{-2}), and at

452   EucFACE LAI matched well in ED2 (1.6 vs. 1.7 m^2 m^{-2}), but was high for LPJ-GUESS (3.2 m^2

453   m^{-2}). At EucFACE LAI ranged from 1.2 to 2.1 over a 28-month measurement period (Duursma

454   et al., (2016), but LPJ-GUESS had very large fluctuations in annual LAI outside of these ranges

455   (Fig. S1). These models are well documented and investigated VDMs, with many studies that

456   have looked into parameter uncertainty (see Supplemental Text A for select references that

457   explore model/parameter sensitivity).

459   Both models displayed nonlinear responses to drought, in concurrence with Hypothesis
460 H1, but they differ in their behavior and between sites. In general, ED2 shows sensitivity to
461 drought duration (Hypothesis H1b), while LPJ-GUESS shows a stronger sensitivity to drought
462 intensity (Hypothesis H1a). ED2's sensitivity to the duration of drought was mild at Palo Verde
463 (Fig. 2a), and stronger at EucFACE particularly during the 4-year drought with a strong non-
464 monotonic pattern (see explanation below) (Fig. 2b). When reporting only percentage of biomass
465 loss, ED2 predicts close to no UCE response at Palo Verde; with a maximum biomass reduction
466 of only 40% during 95% precipitation removal and a 4-year drought event (i.e., UCE). LPJ-
467 GUESS shows very little sensitivity to drought duration but is highly sensitive to drought

468 intensity. C loss predicted by LPJ-GUESS at Palo Verde reached a threshold at ~65% drought
469 intensity, after which forests exhibit strong biomass losses, up to 100% (Fig. 2a). At the
470 EucFACE site, both models predict a critical threshold of biomass loss at 35%-45% drought
471 intensity, with LPJ-GUESS predicting total biomass loss (up to 100%) after this drought
472 intensity threshold (Fig. 2b). The EucFACE drought threshold is lower than that of the
473 seasonally dry mixed tropical forest in Palo Verde.
474   With respect to C loss over a recovering time period (integrated-C-loss), the two models
475 predict similar drought responses at Palo Verde (Fig. 2c), but not at EucFACE (Fig. 2d). At Palo
476 Verde, the similarity between models in integrated-C-loss reflected longer biomass recovery time
477 but less biomass loss in the short-term in ED2 relative to LPJ-GUESS, which predicted greater
478 biomass loss immediately after drought but shorter recovery time. With the exception of the 1-
479 year drought in ED2, both models predict similar integrated-C-loss across a range of UCEs at
480 Palo Verde, via different pathways. The integrated-C-loss metric revealed a strong nonlinear

481 response to drought duration in ED2 (Fig. 2c), while this nonlinearity is less evident when only
482 examining change in biomass (Fig. 2a). The "V"-shaped patterns observed particularly in Fig.
483 2b, arise from interactions between whole-leaf phenology and stomatal responses to drought in
484 ED2. For drought intensities lower than 40%, stomatal conductance is reduced but leaves are not
485 fully shed. Leaf respiration continues, gradually depleting non-structural C pools, followed by a
486 loss of biomass. However, for higher drought intensities, leaf water potentials quickly become
487 systematically lower than leaf turgor loss points and tree cohorts shed all their leaves. This
488 strategy represents an immediate loss of C via leaf shedding, but spares the cohort from slow,
489 respiration-driven depletion of C stocks.

14

492

3.1 Predicted model responses to UCE droughts combined with increased temperature and/or eCO$_2$

Relating to our second hypothesis of additional effects of warming and eCO$_2$, we tested 15 treatments in total, repeating the five climate change scenarios for each of the three drought durations. With the addition of climate change impacts, ED2 remained sensitive to the duration of drought, with warming negatively impacting integrated-C-change and most consistently during 2- and 4-year drought durations. ED2 predicts that during the 2- and 4-year droughts at EucFACE, losses are exacerbated when accompanied with warming, even with eCO$_2$, with 600 ppm having a more detrimental impact than the more elevated 800 ppm (Fig. 3b-c). The average integrated-C-change was -111.0 kg C m^{-2} yr across all 15 treatments (Table 2). Only during the 1-year drought duration did drought plus warming and eCO$_2$ have a buffering effect on C stocks, seen in four out of our five scenarios but only during relatively modest droughts intensities (Fig. 3a; i.e., positive integrated-C-change, see also Table 2).

The ED2 simulations of the seasonally dry Palo Verde site (Fig. 3d-f), produced less frequent negative impacts on drought and climate change driven C losses compared to EucFACE, with an average integrated-C-change of -53.9 kg C m^{-2} yr^{-1} across all 15 treatments (Table 2). During the 2-year drought, applying +2K with eCO$_2$ to 600 ppm showed a slight buffering effect to droughts and the most consistent positive integrated-C-change (Fig. 3e; Table 2). Interestingly, an increase in only eCO$_2$ to 800 ppm (no warming) when applied with the 2- and 4-year droughts resulted in the largest loss in integrated-C-change (Fig. 3e-f), larger than the expected 'most severe' scenario; +2K and 800 ppm.

Similar to ED2, the LPJ-GUESS model showed a nearly complete negative response in integrated-C-change as a result of UCE drought and scenarios of warming and eCO$_2$ at the EucFACE site (Fig. 3g-i), but mixed and more muted results at Palo Verde (Fig. 3j-l, Table 2). The average integrated-C-change relative to the reference case was -95.4 at EucFACE and -7.8 kg C m^{-2} yr at Palo Verde, both less negative compared to ED2. One notable pattern was up until a drought intensity threshold of ~40%, the climate scenarios had no effect or response in integrated-C-change at EucFACE, and the muted response from warming and eCO$_2$ Palo Verde, compared to ED2. Surprisingly, the +2K scenario switched the integrated-C-change to positive, compared to the reference case (Fig. 3g-i; red lines), potentially a physiological process in the

15

Deleted: and

Deleted: 8

Deleted: 6

Deleted: a

527 model to increased temperatures only that signals an anomalous resiliency response. Similar to

528 the results with no climate change, LPJ-GUESS remained sensitive to the intensity of drought,

529 with ~40% precipitation reduction being a threshold.

530   The models and sites differed with regard to SO and MO responses to increasing drought

531 severity and its interactions with warming and eCO_2 (related to conceptual Fig. 1d). ED2 showed

532 a more consistent MO response during UCEs and with additional warming and eCO_2 (Fig. 3;

533 negative integrated-C-change), especially at EucFACE, suggesting these ecosystems will remain

534 in a depressed carbon condition driving vegetation mortality, and/or longer recoveries. LPJ-

535 GUESS produced more opportunities for SO with climate change. For example, at EucFACE

536 CO_2 fertilization created small SO periods that then led to MO with increasing drought severities,

537 and at Palo Verde all +2K and 600 ppm led to a SO (Fig. 3j-l; Table 2).

538   Both models predicted that C losses due to drought interactions with increased

539 temperature and eCO_2 were less severe at the seasonally dry Palo Verde site compared to the

540 somewhat less seasonal, more humid EucFACE site (Table 2), which could be attributed to

541 higher diversity in PFT physiology at Palo Verde. Palo Verde's community composition that

542 emerged following drought included either three (LPJ-GUESS) or four (ED2) PFTs, while only a

543 single PFT existed at EucFACE. With rising temperatures under climate change, UCEs will be

544 hotter and drier. Nine out of the twelve simulations with both +2K and 600 ppm CO_2, and all but

545 one +2K and 800 ppm CO_2 produced a negative integrated-C-change, implying stronger C losses

546 and/or longer recovery times when droughts are exacerbated by increasing temperatures (Table

547 2).

548

549 **4 Discussion**

550   Vegetation demographic models (VDMs) allowed us to uniquely explore two hypotheses

551 regarding a range of modeled response of terrestrial ecosystems to unprecedented climate

552 extremes (UCEs), and setting the stage for the following perspectives to help guide future

553 research. Key model results include strong nonlinearities (Hypothesis H1) in C response to

554 extreme drought *intensities* in LPJ-GUESS and alternatively drought *durations* in ED2 (at one of

555 two sites), with differences in thresholds between the two models and ecosystems. These

556 nonlinearities may arise from multiple mechanisms that we begin to investigate here, including

557 shifts in plant hydraulics or other functional traits, C allocation, phenology, stand size-structure

Deleted: and

16

559 and/or age demography, and compositional changes, all which vary among ecosystem types. A

560 critical look of driving model mechanisms, which emerged from the hypothetical drought

561 simulations used here, are summarized in Table 3. The models also show exacerbated biomass

562 loss and recovery times in the majority of our scenarios of warming and eCO$_2$, supporting

563 Hypothesis H2. Below, we discuss the underlying mechanisms that drive simulated ecosystem

564 response to UCEs using the models and sites as conceptual "experimental tools" and

565 observational evidence from the literature. We focus on two temporal stages of the UCE: The

566 pre-drought ecosystem stage characterized as the quasi-stable state of the ecosystem prior to a

567 UCE, which can mediate ecosystem resistance and disturbance impact, and the post-drought

568 recovery stage (Table 1).

569

570 **4.1 The role of ecosystem processes and states prior to UCEs**

571 **4.1.1 The role of phenology and phenological strategies prior to UCEs:**

572   Observations show that diversity of deciduousness contributes to successful alternative

573 strategies for tropical forest response to water stress (Williams et al., 2008). For example, during

574 the severe 1997 El Nino drought, brevi-deciduous trees and deciduous stem-succulents within a

575 tropical dry site in Guanacaste Costa Rica retained leaves during the extreme wet-season

576 drought, behaving differently than during normal dry seasons (Borchert et al., 2002). Both

577 models here predict that neither seasonal deciduousness, nor drought-deciduous phenology at the

578 seasonally dry tropical forest, Palo Verde (which consists of trees with different leaf

579 phenological strategies), act to buffer the forest from a large drop in LAI during UCEs (Fig. S1a-

580 b). Even with this large decrease in LAI, ED2 predicted a very weak biomass loss at the time of

581 UCEs (Fig. 2a), suggesting large-scale leaf loss is not a direct mechanism of plant mortality in

582 ED2. Leaf loss is one component of total carbon turnover flux equations in terrestrial models, in

583 addition to woody loss, fine-roots, and reproductive tissues. Having a better understanding of

584 when extreme levels of phenological turnover contribute to stand-level mortality could be

585 improved. Among other turnover hypothesis explored, Pugh et al. (2020) found that phenological

586 turnover fluxes where just as important as mortality fluxes in driving forest turnover time in the

587 VDMs: LPJ-GUESS, CABLE-POP, ORCHIDEE, but not the LSM JULES. At the EucFACE

588 site prior to the simulated extreme drought, LPJ-GUESS displayed strong inter-annual variability

Deleted: LAI was stable in ED2, while

17

590   in LAI (Fig. S1a-b). This capability of large swings in LAI (5.8 to 0.8) by LPJ-GUESS could

591   contribute to model uncertainty and the considerable mortality response at EucFACE. Modeled

592   LAI was the largest source of variability in another ecosystem model, CABLE, when evaluating

593   the simulated response to CO_2 fertilization (Li et al., 2018). VDMs could be improved by better

594   capturing different plant phenological responses to UCEs by better representing a range of leaf-

595   level morphological and physiological characteristics relevant to plant-water relations such as

596   leaf age, retention of young leaves even during extreme droughts, (Borchert et al., (2002)), and

597   variation in hydraulic traits as a function of leaf habit (Vargas et al., (2021)) (Table 3). Two such

598   examples are seen in the FATES model where the possibility for "trimming" the lowest leaf

599   layer can occur when leaves are in negative carbon balance due to light limitation thus

600   optimizing maintenance costs and carbon gain, as well as leaf age classifications providing

601   variations in leaf productivity and turnover.

602

603   **4.1.2 The role of plant hydraulics prior to UCEs:**

604   Susceptibility of plants to hydraulic stress is one of the strongest determinants of

605   vulnerability to drought, with loss of hydraulic conductivity being a major predictor of drought

606   mortality in temperate (McDowell et al., 2013; Anderegg et al., 2015; Sperry and Love, 2015;

607   Venturas et al., 2021) and tropical forests (Rowland et al., 2015; Adams et al., 2017b), as well as

608   a tractable mortality mechanism to represent in process-based models (Choat et al., 2018,

609   Kennedy et al., 2019). Both LPJ-GUESS and ED2 exhibited a wide range in amount and pattern

610   of plant-available-water prior to drought (Fig. S1c-d), contributing to large differences in UCE

611   response. LPJ-GUESS, which does not simulate hydrodynamics, predicted lower total plant-

612   available-water at both sites compared to ED2, and subsequently simulated greater mortality and

613   a greater increase in plant-available-water right after the UCEs as a result of less water demand.

614   Due to ED2 using a static mortality threshold from conductivity loss (88%), it likely does not

615   accurately reproduce the wide range of observations of drought-induced mortality. In ED2, large

616   trees, with longer distances to transport water, were at higher risk and suffered higher mortality

617   (Fig. 4), demonstrating how stand demography, size structure, and tapering of xylem conduits

618   can play an important role in ecosystem models (Petit et al., 2008; Fisher et al., 2018). Of the

619   VDMs that are beginning to incorporate a continuum of hydrodynamics (e.g., ED2 (described in

620   Methods 2.1 section) and FATES-HYDRO (Fang et al., 2022, based on Christoffersen et al.,

18

630   2016), they are able to solve for transient water from soils to roots, through the plant and connect

631   with transpiration demands. Therefore instead of the plant water stress function being based on

632   soil water potentials, it is replaced with more realistic connections with leaf water potentials.

633   Mortality is then caused by hydraulic failure via embolism controlled by the critical water

634   potential (P_{50}) that leads to 50% loss of hydraulic conductivity. For advancements in tree level

635   hydrodynamic modeling see the FETCH3 model (Silva et al., 2022), for justification for plant

636   hydrodynamics in conjunction with multi-layer vertical canopy profiles see Bonan et al., (2021).

637   There are strong interdependencies and related mechanisms connecting both hydraulic failure

638   (e.g., low soil moisture availability) and C limitation (e.g., stomatal closure) during drought

639   (McDowell et al., 2008; Adams et al., 2017b), and these interactions should be incorporated in

640   ecosystem modeling and further explored (Table 3).

641   **4.1.3. The role of carbon allocation prior to UCEs:**

642   Plants have a variety of strategies to buffer vulnerability to water and nutrient stress

643   caused by extreme droughts, such as allocating more C to deep roots (Joslin et al., 2000; Schenk

644   and Jackson, 2005), investing in mycorrhizal fungi (Rapparini and Peñuelas, 2014), or reducing

645   leaf area without shifting leaf nutrient content (Pilon et al., 1996). Alternatively, presence of

646   deep roots doesn't necessarily lead to deep soil moisture utilization, as seen in a 6-year

647   Amazonian throughfall exclusion experiment where deep root water uptake was still limited,

648   even with high volumetric water content (Markewitz et al., 2010). Elevated CO_2 alone will

649   enhance growth and water-use efficiency (Keenan et al., 2013), reducing susceptibility to

650   drought. However, such increased productivity within a forest stand, and associated structural

651   overshoot during favorable climate windows, can also be reversed by increased competition for

652   light, nutrients, and water during unfavorable UCEs – potentially leading to mortality overshoot

653   (Fig. 1d) and higher C loss. Mortality overshoot, as a result of structural overshoot, could be an

654   explanation for the negative integrated-C-change (i.e., C loss) in the majority of eCO2-only

655   simulations (18 out of 24 scenarios; Table 2).

656   Effects of CO_2 fertilization on plant C allocation strategies are uncertain. As a result,

657   ecosystem models differ in their assumptions on controls of C allocation in response to eCO2,

658   leading to divergent plant C use efficiencies (Fleischer et al., 2019). Global scale terrestrial

659   models are beginning to include optimal dynamic C allocation schemes, over fixed ratios, that

660   account for concurrent environmental constraints on plants, such as water, and adjust allocation

19

661 based on resource availability such as in LM3-PPA (Weng et al., 2015), but the representation of

662 C allocation is still debated and progressing (De Kauwe et al., 2014; Montané et al., 2017; Reyes

663 et al., 2017). Options for carbon allocation strategies can based on the allometric partitioning

664 theory (i.e., allocation follows a power allometry function between plant size and organs which

665 is insensitive to environmental conditions; Niklas, 1993), as an alternative to ratio-based optimal

666 partitioning theory (i.e., allocation to plant organs based on the most limiting resources)

667 (McCarthy and Enquist, 2007) or fixed ratios (Table 3), and the strategies should be further

668 investigated particularly due to VDMs substantial use of allometric relationships. A meta-

669 analysis of 164 studies found that allometric partitioning theory outperformed optimal

670 partitioning theory in explaining drought-induced changes in C allocation (Eziz et al., 2017).

671 Further eco-evolutionarily-based approaches such as optimal response or game-theoretic

672 optimization, as well as entropy-based approaches are useful when wanting to simulate higher

673 levels of complexity (reviewed in Franklin et al. 2012). With more frequent UCEs and the need

674 for plants to reduce water consumption, a shift in the optimal strategy of allocation between

675 leaves and fine roots should change. The goal functions (e.g., fitness proxy) used in optimal

676 response modeling can account for these shifts in costs and benefits of allocation between all

677 organs (Franklin et al. 2009, 2012).

678

679 **4.1.4 The role of plant carbon storage prior to UCEs:**

680   Studies of neotropical and temperate seedlings show that pre-drought storage of non-

681 structural carbohydrates (NSCs) provides the resources needed for growth, respiration

682 osmoregulation, and phloem transport when stomata close during subsequent periods of water

683 stress (Myers and Kitajima, 2007; Dietze and Matthes, 2014; O'Brien et al., 2014). Furthermore,

684 direct correlations have been shown between NSC depletion and embolism accumulation, and

685 the degree of pre-stress reserves and utilization of soluble sugars (Tomasella et al., 2020). The

686 amount of NSC storage required to mitigate plant mortality during C starvation and interactions

687 with hydraulic failure from severe drought is difficult to quantify, due to the many roles of NSCs

688 in plant function and metabolism (Dietze and Matthes, 2014). For example, NSCs were not

689 depleted after 13 years of experimental drought in the Brazilian Amazon (Rowland et al., 2015).

690 As atmospheric CO_2 increases with climate change, NSC concentrations may increase, as seen in

691 manipulation experiments (Coley, 2002), but interactions with heat, water stress, enhanced leaf

Deleted: ; Zhu et al., 2019

Deleted: It is worth investigating the differences between

Deleted: C

695　shedding, and nutrient limitation complicates this relationship, and needs to be further explored.

696　Despite the recognition of the critical role that plant hydraulic functioning and NSCs play in tree

697　resilience to extremes, knowledge gaps and uncertainties preclude fully incorporating these

698　processes into ecosystem models.

699　　　　Compared to ED2, LPJ-GUESS predicted low plant carbon storage (a model proxy for

700　NSCs) prior to and during drought, and at times became negative, thereby creating C costs (Fig.

701　S2a-b), leading to C starvation and potentially explaining the larger biomass loss in LPJ-GUESS

702　at both sites. Alternatively, ED2 maintained higher levels of NSCs providing a buffer to stress,

703　and mitigating the negative effects of drought. Maintenance of NSCs in ED2, even during

704　prolonged drought (at EucFACE) is due to: (1) trees resorbing a fraction of leaf C during leaf

705　shedding, (2) no maintenance costs for NSC storage in the current version, and (3) no allocation

706　of NSCs to structural growth until NSC storage surpasses a threshold (the amount of C needed to

707　build a full canopy of leaves and associated fine roots), allowing for a buffer to accumulate. In

708　LPJ-GUESS, accumulation and depletion of NSC is recorded as a 'C debt' being paid back in

709　later years. The contrasting responses of the two models to drought, and the likely role of NSCs

710　in explaining differences in model behavior, highlights the need to better understand NSC

711　dynamics and to accurately represent the relevant processes in models (Richardson et al., 2013;

712　Dietze and Matthes, 2014). More observations of C accumulation patterns and how/where NSCs

713　drive growth, respiration, transport and cellular water relations would enable a more realistic

714　implementation of NSC dynamics in models (Table 3).

715

716　**4.1.5 Role of functional trait diversity prior to UCEs:**

717　　　　Currently LPJ-GUESS simulates the Palo Verde community using three PFTs, while ED2 uses

718　four PFTs that differ in photosynthetic and hydraulic traits. The community composition simulated by

719　ED2 is shown to be more resistant to UCEs compared to LPJ-GUESS (Fig. 5), perhaps due to

720　relatively higher functional diversity (via more PFTs with additional phenological and hydraulic

721　diversity). This additional diversity helps to buffer ecosystem response to drought by allowing more

722　tolerant PFTs to benefit from reductions in less-tolerant PFTs, thus buffering reductions in ecosystem

723　function (Anderegg et al., 2018). Higher diversity ecosystems were found to protect individual species

724　from negative effects of drought (Aguirre et al., 2021) and enhance productivity resilience following

725 wildfire (Spasojevic et al., 2016); thus, functionally diverse communities may be key to enhancing
726 tolerance to rising environmental stress.
727   Recent efforts to consolidate information on plant traits (Reich et al., 2007; Kattge et al., 2011)
728 have contributed to identifying relationships that can impact community-level drought responses
729 (Skelton et al., 2015; Anderegg et al., 2016a; Uriarte et al., 2016; Greenwood et al., 2017), such as
730 life-history characteristics, and strategies of resource acquisition and conservation as predictors of
731 ecosystem resistance (MacGillivray et al., 1995; Ruppert et al., 2015). While adding plant trait
732 complexity in ESMs may be required to accurately simulate key vegetation dynamics, it necessitates
733 more detailed parameterizations of processes that are not explicitly resolved (Luo et al., 2012). Further
734 investigation of how VDMs represent interactions leading to functional diversity shifts is crucial to
735 this issue. Enquist and Enquist, (2011), as an example, show that long-term patterns of drought (20-
736 years) have led to increases in drought-tolerant dry forest species, which could modulate resistance to
737 future droughts. Higher diversity of plant physiological traits and drought-resistance strategies is
738 expected to enhance community resistance to drought, and models should account for shifts in diverse
739 functionality (Table 3).

740

741 **4.2 The role of ecosystem processes and states in post-UCE recovery**

742 **4.2.1 The role of soil water resources post-UCEs:**

743   Our simulation results generally demonstrated a fast recovery of plant-available-water
744 and LAI at both sites (Fig. S1). Annual plant-available-water substantially increased right after
745 drought by an average of 163 mm at Palo Verde and 213 mm at EucFACE in the LPJ-GUESS
746 simulations, compared to much lower increases in ED2 (50 mm and 12 mm at Palo Verde and
747 EucFACE). This increase in available water post-drought can be attributed to reduced stand
748 density and water competition (Fig. S2c-d; diamonds vs. circles), alleviating the demand for soil
749 resources (water) and subsequent stress, which has also been shown in observations (McDowell
750 et al., 2006; D'Amato et al., 2013). After large canopy tree mortality events there can be
751 relatively rapid recovery of forest biogeochemical and hydrological fluxes (Biederman et al.,
752 2015; Anderegg et al., 2016b; Biederman et al., 2016). These crucial fluxes strongly influence
753 plant regeneration and regrowth, which can buffer ecosystem vulnerability to future extreme
754 droughts. However, this enhanced productivity has a limit. In a scenario where UCEs continue to

22

755 intensify, causing greater reductions in soil water and reduced ecosystem recovery potential, the
756 SO growth that typically occurs after UCEs may be dampened (Fig. 1d). In water-limited
757 locations, similar to the dry forest sites used here, initial forest recovery from droughts were
758 faster due to thinning induced competitive-release of the surviving trees, and shallow roots not
759 having to compete with neighboring trees for water, allowing for more effective water user
760 (Tague and Moritz, 2019), stressing the importance of root competition and distribution in
761 models (Goulden and Bales, 2019). Tague and Moritz, (2019) also reported that this increased
762 water use efficiency and SO ultimately lead to water stress and related declines in productivity,
763 similar to the MO concept (Jump et al., 2017; McDowell et al., 2006). Since a core strength of
764 VDMs is predicting stand demography during recovery, improved quantification of density-
765 dependent competition following stand dieback would be beneficial for model benchmarking
766 (Table 3).

767

768 **4.2.2 The role of lagged turnover and secondary stressors post-UCEs:**

769   Time lags in forest compositional response and survival to drought could indicate
770 community resistance or shifts to more competitive species and competitive exclusion. During a
771 15-year recovery period from extreme drought at Palo Verde, LPJ-GUESS predicted an increase
772 in stem density (stems m^2 yr^{-1}) (Fig. S2c) compared to ED2, which predicted almost no impact in
773 stem recovery. The mortality "spike" in ED2 due to drought was muted and slightly delayed,
774 contributing to ED2's lower biomass loss and more stable behavior of plant processes over time
775 at Palo Verde. At EucFACE, both models exhibited a pronounced lag effect in stem turnover
776 response, i.e. ~8-12 years after drought (Fig. S2d). After about a decade, strong recoveries and
777 increased stem density occurred, which in ED2 was followed by delayed mortality/thinning of
778 stems. Delayed tree mortality after droughts is common due to optimizing carbon allocation and
779 growth (Trugman et al., 2018), but typically only up to several years post-drought, not a decade
780 or more as seen in the model.

781   The versions of the VDMs used here do not directly consider post-drought secondary
782 stressors such as infestation by insects or pathogens, and the subsequent repair costs due to stress
783 damage, which could substantially slow the recovery of surviving trees. Forest ecologists have
784 long recognized the susceptibility of trees under stress, particularly drought, to insect attacks and

23

785   pathogens (Anderegg et al., 2015). Tight connections between drought conditions and increased

786   mountain pine beetle activity have been observed (Chapman et al., 2012; Creeden et al., 2014),

787   and can ultimately lead to increased tree mortality (Hubbard et al., 2013). Leaf defoliation is a

788   major concern from insect outbreaks following droughts, and can have large impacts on C

789   cycling, plant productivity, and C sequestration (Amiro et al., 2010; Clark et al., 2010; Medvigy

790   et al., 2012). Implementing these secondary stressors in models could slow the rate of post-UCE

791   recovery and lead to increased post-UCEs tree mortality.

792

4.2.3 The role of stand demography post-UCEs:

794   Change in stand structure is an important model process to capture, because large trees

795   have important effects on C storage, community resource competition, and hydrology

796   (Wullschleger et al., 2001) (Table 3), and maintaining a positive carbohydrate balance is

797   beneficial in sustaining (or repairing) hydraulic viability (McDowell et al., 2011). There is

798   increasing evidence, both theoretical (McDowell and Allen, 2015) and empirical (Bennett et al.,

799   2015; Rowland et al., 2015; Stovall et al., 2019), that large trees (particularly tall trees with high

800   leaf area) contribute to the dominant fraction of dead biomass after drought events. Under rising

801   temperatures (and decreasing precipitation), VPD will increase, leading to a higher likelihood of

802   large tree death (Eamus et al., 2013; Stovall et al., 2019), driving MO events as hypothesized in

803   Fig. 1d. Consistent with this expectation, ED2 predicted that the largest trees (>100 cm)

804   experienced the largest decreases in basal area to compared to all other size classes (Fig. 4). This

805   drought-induced partial dieback and mortality of large dominant trees has substantial impacts on

806   community-level C dynamics, as long-term sequestered C is liberated during the decay of new

807   dead wood (Palace et al., 2008; Potter et al., 2011). In ED2, the intermediate size class (60 - 80

808   cm) increased in basal area following large-tree death, taking advantage of the newly open

809   canopy space. However, small size classes do not necessarily benefit from canopy dieback. For

810   example, in a dry tropical forest, prolonged drought led to a decrease in understory species and

811   small-sized stems (Enquist and Enquist, 2011).

812   Due to VDMs being able to exhibit dynamic biogeography they are more useful at

813   predicting shifts in community composition beyond LSMs capabilities. Further areas of

814   advancement (described in Franklin et al. (2020)) is including models of natural selection, self-

815   organization, and entropy maximization which can substantially improve community dynamic

Deleted: whole-tree

Deleted: stand

24

818 responses in varying environments such as UCEs. Eco-evolutionary optimality (EEO) theory can
819 also help improve functional trait representation in global process-based models (reviewed in
820 Harrison et al., 2021), through hypotheses in plant trait trade-offs and mechanistic links between
821 processes such as resource demand, acquisition, and plant's competitiveness and survival; traits
822 associated with high degrees of sensitivity in models. The power of prognostic VDMs to predict
823 shifts in demography and community migration with climate change is large, but rarely is being
824 constrained with plant-level EEO theory, and thus will likely need to use stand level competition
825 and coexistence principles of how plants self-organize (Franklin et al. 2020).

826

4.2.4 The role of functional trait diversity & plant hydraulics post-UCEs:

828   In field experiments, higher disturbance rates have shifted the recovery trajectory and

> Deleted: During the recovery phase from
> Deleted: , competition
> Deleted: will likely

829 competition of the plant community towards one that is composed of opportunistic, fast-growing
830 pioneer tree species, grasses (Shiels et al., 2010; Carreño-Rocabado et al., 2012), and/or
831 deciduous species, as also seen in model results (Hickler et al., 2004). In the treatments presented

> Deleted: previous

832 here, deciduous PFT types were also the strongest to recover after 15 years in both models,
833 surpassing pre-drought values (Fig. 5). It should be noted that ED2 exhibited a strong recovery in
834 the evergreen PFT as well, inconsistent with the above literature (Fig. 5b). PFTs in ED2 respond

> Deleted: (over two other deciduous PFT types)

835 to drought conditions via stomatal closure and leaf shedding, buffering stem water potentials
836 from falling below a set mortality threshold (i.e., 88% of loss in conductivity). This conductivity
837 threshold may need to be reconsidered if further examination reveals an unrealistic advantage
838 under drought conditions for evergreen trees, which exhibited a lower impact from droughts
839 (compared to deciduous and brevi-deciduous PFTs) in ED2. Nitrogen cycling feedbacks were
840 not investigated here, but could also be an explanation for a strong evergreen PFT recovery.

841   Recovery of surviving trees could be hindered by the high cost of replacing damaged
842 xylem associated with cavitation (McDowell et al., 2008; Brodribb et al., 2010). Many studies
843 have identified "drought legacy" effects of delayed growth or gross primary productivity
844 following drought (Anderegg et al., 2015; Schwalm et al., 2017) and the magnitude of these
845 legacies across species correlates with the hydraulic risks taken during drought itself (Anderegg
846 et al., 2015). The conditions under which xylem can be refilled remain controversial, but it seems
847 likely that many species, particularly gymnosperms, may need to entirely replace damaged

853 xylem (Sperry et al., 2002), and trees worldwide operate within narrow hydraulic safety margins,

854 suggesting that trees in all biomes are vulnerable to drought (Choat et al., 2012). The amount of

855 damaged xylem from a given drought event and recovery rates also vary across trees of different

856 sizes (Anderegg et al., 2018).

857   Plasticity in nutrient acquisition traits, intraspecific variation in plant hydraulic traits

858 (Anderegg et al., 2015), and changes in allometry (e.g., Huber values) can have large effects on

859 acclimation to extreme droughts. This suggests some capacity for physiological adaptation to

860 extreme drought, as seen by short-term negative effects from drought and heat extremes being

861 compensated for in the longer term (Dreesen et al., 2014). Still, given the shift towards more

862 extreme droughts with climate change, vegetation mortality thresholds are likely to be exceeded,

863 as reported in Amazonian long-term plots where mortality of wet-affiliated genera has increased

864 while simultaneously new recruits of dry-affiliated genera are also increasing (Esquivel-Muelbert

865 et al., 2019). Increasing occurrences of heat events, water stress and high VPD will lead to

866 extended closure of stomata to avoid cavitation, progressively reducing CO_2 enrichment benefits

867 (Allen et al., 2015). Where CO_2 fertilization has been seen to partially offset the risk of

868 increasing temperatures, the risk response was mediated by plant hydraulic traits (Liu et al.,

869 2017) using a soil–plant–atmosphere continuum (SPAC) model, yet interactions with novel

870 extreme droughts were not considered. The VDM simulations suggest that the combination of

871 elevated warming and potential structural overshoot from eCO_2 (or inaccurate representation in

872 NSCs allocation/usage priority) will exacerbate consequences of UCEs by reductions in both C

873 stocks and post-drought biomass recovery speeds (Fig. 3). Therefore, future UCE recovery may

874 not be easily predicted from observations of historical post-disturbance recovery. An associated

875 area for further investigation is to better understand the hypothesized interplay between

876 amplified mortality from hotter UCEs followed by structural overshoot regrowth during wetter

877 periods (Fig. 1d), which could potentially lead to continual large swings in MO and SO and

878 vulnerable net ecosystem C fluxes through time (Table 3).

879

880 **5 Summary of perspectives for model advancement**

881   Model limitations and unknowns exposed by our simulations and literature review

882 highlight current challenges in our ability to understand and forecast UCE effects on ecosystems.

883 These limitations reflect a general lack of empirical experiments focused on UCEs. Insufficient

26

884 data means that relevant processes may currently be poorly represented in models, and models

885 may then misrepresent C losses during UCEs. The two VDMs used here had different

886 sensitivities to drought duration and intensity. These model uncertainties could potentially be

887 addressed by improved datasets on thresholds of conductivity loss at high drought intensities, the

888 role of trait diversity (e.g., different strategies of drought deciduousness and EEO theory) in

889 buffering ecosystem drought responses, and a better grasp of allocation to plant C storage stocks

890 before, during, and after multi-year droughts. Our study takes some initial steps to identify and

891 assess model gaps in terms of mechanisms and magnitudes of responses to UCEs, which can

892 then be used to inform and develop field experiments targeting key knowledge gaps as well as to

893 prioritize ongoing model development (Table 3). Our intention was not to do an exhaustive list

894 of UCE simulation experiments, and additional modeling perturbations and experiments would

895 be useful outcomes of future studies. For example, we begin to investigate duration of droughts

896 but we did not consider frequency of back-to-back UCEs. This iterative model-experiment

897 framework of using VDMs as hypothesis testing tools offers strong potential to drive progress in

898 improving our understanding of terrestrial ecosystem responses to UCEs and climate feedbacks,

899 while informing the development of the next generation of models.

Deleted: uncertainties

Deleted: outstanding

27

946 **Table 1.** Hypothesized plant processes and ecosystem state variables affecting pre-drought

947 resistance and post-drought recovery in the context of unprecedented climate extremes (UCEs).

948 The "Included in Model?" column indicates which processes or state variables are represented in

949 each of the two models studied in this paper. The mechanisms listed in the two right columns

950 refer to real-world ecosystems and are not necessarily represented in the ED2 and LPJ-GUESS

951 models. Contents of the table are based on a non-exhaustive literature review, expert knowledge,

952 and modeling results presented here. Symbols refer to the following literature sources: *

953 Borchert et al., 2002; Williams et al., (2008); ** Dietze and Matthes, (2014); O'Brien et al.,

954 2014; *** ENQUIST and ENQUIST, (2011); Greenwood et al., (2017); Powell et al., (2018); ^

955 Rowland et al., (2015); McDowell et al., (2013); Anderegg et al., (2015); ^^ Joslin et al., 2000;

956 Markewitz et al., (2010); ^^^ Powell et al., (2018); ^^^^ Bennett et al., (2015); Rowland et al.,

957 (2015); ~ Hubbard et al., (2013); ~~ McDowell et al., (2006); D'Amato et al., (2013); + Zhu et

958 al., (2018); Vargas et al., (2021); % Trugman et al., (2019); %% Franklin et al., (2012); %%

959 Franklin et al., (2020).

Process or State Variable	Included in model?	Mechanisms affecting pre-UCE drought resistance influencing impact	Mechanisms affecting post-UCE drought recovery
Processes			
1) Phenology Schemes	ED2: Yes LPJ-G: Yes	- Leaf area and metabolic activity modulates vulnerability to death - Drought-deciduousness reduces vulnerability to drought *, with higher water potential at turgor loss point and less leaf vulnerability to embolism [+]	- Leaf lifespan tends to increase from pioneer to late-successional species in some ecosystems (e.g., tropical forests) and is a balance between C gain and its cost
2) Plant Hydraulics	ED2: Yes LPJ-G: No	- Cavitation resistance traits ^ - Turgor loss, hydraulic failure (stem embolism) lead to increased plant mortality and enhanced vulnerability to secondary stressors.	- Replacement cost of damaged xylem slows recovery of surviving trees
3) Dynamic Carbon Allocation	ED2: Yes LPJ-G: Yes	- Increased root allocation could offset soil water deficit under gradual onset of drought ^^ - Leaf C allocation strategies should be connected to hydraulic processes [%]	- Allocation among fine roots, xylem, & leaves affects recovery time & GPP/LAI trajectory - Eco-evolutionary optimality theory [%%]

4) Non-Structural Carbohydrate (NSC) Storage	ED2: Yes LPJ-G: Yes	- NSCs buffer C starvation mortality due to reduced primary productivity. - Maintenance of hydraulic function & avoiding hydraulic failure **	- Low NSC could increase vulnerability to secondary stressors during recovery
State Variables			
1) Plant-Soil Water Availability	ED2: Yes LPJ-G: Partly	- Low soil water potential increases risk of tree C starvation, turgor loss and hydraulic failure	- After stand dieback reduced demand for soil resources &/or reduced shading - Increased soil water enhances regeneration/ regrowth, buffers vulnerability to long-term drought ~ ~
2) Plant Functional Diversity	ED2: Yes LPJ-G: Yes	- Presence of drought-tolerant species modulates resistance at community level. - Shallow-rooting species more vulnerable ^^^ ***	- Changed resource spectra shift competitive balance in favor of grasses and pioneer trees
3) Stand Demography	ED2: Yes LPJ-G: Yes	- Larger tree size enhances vulnerability to drought and secondary stressors due to higher maintenance costs ^^^^	- Mortality of canopy individuals favors understory species and smaller size-classes - Self-organizing principles %%%
4) Compounding Stressors	ED2: No LPJ-G: No	- Reduced resistance to insects and pathogens due to physiological/mechanical/ hydraulic damage & depletion of NSC	- Infestation by insects and pathogens, repair of damage due to secondary stressors, slows recovery of surviving trees ~

964

Table 2 Impact of eCO_2 and/or temperature on the integrated-C-change (kg C m^{-2} yr) relative to drought treatments with no additional warming or eCO_2, for both models, and both sites seen in Fig. 3. Quantified as average and minimum integrated-C-change across all 20 drought intensities for step-change scenarios of warming and eCO_2. The percentage of each scenario that was negative in integrated-C-change (i.e., decreases in C loss). Green values represent positive integrated-C-change.

EucFACE		ED2			LPJ-GUESS		
		Average integrated C change	Largest integrated C change	% climate scenario was negative	Average integrated C change	Largest integrated C change	% climate scenario was negative
1 year	600 ppm	2.2	0.0	33.3	-74.6	-396.6	36.8
	800 ppm	-10.6	-73.0	50.0	-124.1	-416.0	57.9
	2K	2.3	-0.5	16.7	21.3	-20.8	15.8
	2K, 600 ppm	0.5	-8.2	61.1	-67.5	-201.5	78.9
	2K, 800 ppm	1.8	-0.4	22.2	-145.9	-400.1	47.4
2 year	600 ppm	-105.6	-456.7	77.8	-85.2	-260.6	63.2
	800 ppm	-199.0	-522.9	83.3	-106.3	-350.1	42.1
	2K	-10.3	-34.7	77.8	14.2	-35.2	31.6
	2K, 600 ppm	-204.9	-666.1	77.8	-47.6	-128.8	84.2
	2K, 800 ppm	-12.4	-61.6	50.0	-167.0	-421.9	68.4
4 year	600 ppm	-125.5	-306.2	83.3	-122.6	-277.4	94.7
	800 ppm	-277.1	-423.3	100.0	-212.2	-523.7	89.5
	2K	-61.8	-188.6	72.2	12.9	-13.8	31.6
	2K, 600 ppm	-385.9	-674.2	94.4	-79.1	-197.3	94.7
	2K, 800 ppm	-277.9	-737.7	72.2	-247.0	-503.8	100.0
Average		-111.0	-277.0	64.8	-95.4	-276.5	62.5
Palo Verde		ED2			LPJ-GUESS		
1 year	600 ppm	-1.6	-6.2	77.8	-11.0	-32.4	78.9
	800 ppm	6.7	-0.2	11.1	-39.2	-154.0	100.0
	2K	-1.0	-15.3	38.9	-33.4	-75.1	100.0
	2K, 600 ppm	2.5	-1.1	22.2	6.5	-4.6	52.6
	2K, 800 ppm	-6.6	-16.6	77.8	-121.1	-237.7	100.0
2 year	600 ppm	15.1	-16.7	38.9	27.3	-6.0	10.5
	800 ppm	-229.2	-756.6	66.7	20.6	-17.2	26.3
	2K	-8.2	-71.8	50.0	32.0	-12.7	15.8
	2K, 600 ppm	24.8	-5.7	11.1	36.2	-1.2	5.3
	2K, 800 ppm	-152.9	-348.1	77.8	8.0	-54.5	36.8
4 year	600 ppm	-11.1	-37.3	94.4	3.4	-25.1	26.3
	800 ppm	-260.2	-694.8	94.4	-25.2	-132.6	57.9
	2K	-39.0	-133.8	66.7	-7.7	-45.9	68.4
	2K, 600 ppm	1.0	-16.4	38.9	6.1	-4.1	31.6
	2K, 800 ppm	-148.5	-429.3	83.3	-20.0	-75.5	78.9
Average		-53.9	-170.0	56.7	-7.8	-58.6	52.6

972 **Table 3** Summary of suggested critical look of driving mechanisms (e.g., ecosystem or plant

973 processes and state variables), which emerged from the hypothetical drought simulations used

974 here to explore for future research in manipulation experiments, data collection, and model

975 development and testing, as related to furthering our understanding of UCE resistance and
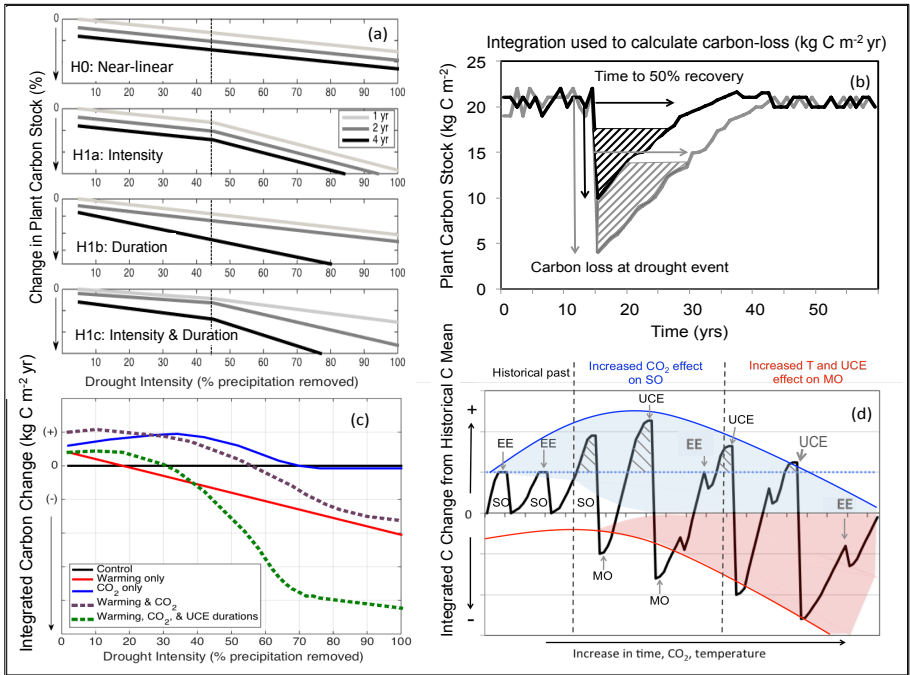
976 recovery.

UCE Drought Resistance & Recovery Summary	
Processes	**Suggestions of driving mechanisms to further explore in data and models**
1) Phenology Schemes	Represent morphological and physiological traits relevant to plant-water relations; drought- deciduousness can reduce vulnerability to drought; phenology of evergreens needs more investigation.
2) Plant Hydraulics	Interactions between hydraulic failure (e.g. low soil moisture availability) and C limitation (e.g. stomatal closure) during drought should be included in models. Account for turgor loss, hydraulic failure traits, costs to recover damaged xylem.
3) Dynamic Carbon Allocation	C allocation based on eco-evolutionary optimality (EEO) and allometric partitioning theory in addition, or replacing ratio-based optimal partitioning theory, and fixed ratios. Explore root allocation that could offset soil water deficits.
4) Non-structural Carbohydrate (NSC) Storage	Deciding best practices for NSC representation in models. Better understanding of NSC storage required to mitigate plant mortality during C starvation and interactions with avoiding hydraulic failure during severe droughts.
States Variables	
1) Plant-Soil Water Availability	Better quantification of the amount and accessibility of plant-available water for surviving trees, and tradeoff between increased structural productivity but vulnerability to subsequent droughts. Future relevance, or benefit, of lower water demand due to thinning with UCEs.
2) Plant Functional Diversity	Understand how higher diversity of plant physiological traits and drought-resistance strategies will enhance community resistance to drought; models still need to account for shifts in diverse functionality, including deciduousness shifts and interplay of regrowth structural overshoot followed by amplified mortality from hotter UCEs.
3) Stand Demography	Large trees more vulnerable to drought; need data on changes in C stock with UCEs in high-density smaller tree stands vs. stands with larger trees. Using 'self-organization' principles for modeling stand level competition and coexistence under UCEs.

977

Deleted: ions

Deleted: ing

Deleted: of the driving mechanisms (e.g., ecosystem or plant processes and state variables)

Deleted: the

Figure 1 Conceptual diagrams showing impacts of extreme droughts (unprecedented climate extremes, UCEs; i.e., record-breaking droughts) on plant C stocks. (a) **Conceptual response diagram**: potential loss in C stock as a function of increasing drought intensity (0-100% precipitation removal) and drought duration (1, 2 or 4 years of drought). In this example, an arbitrary threshold of 45% precipitation reduction and 4-year drought duration is assumed to correspond to a UCE. The "null hypothesis" (H0, top panel) is a near-linear response of C stocks to droughts. Alternative hypotheses include nonlinear and threshold responses to drought intensity (H1a), drought duration via different slope responses (H1b), and combined effects of both drought intensity and durations (H1c). (b) **Conceptualized UCE C loss diagram**: responses of forest C stocks to a large (grey) and small (black) UCE. "Integrated-C-loss" (kg C m^{-2} yr) denotes the integral of the C loss over time and is calculated from the two arrows: the total loss in C (kg C m^{-2}) due to drought, and the time (yr) to recover 50% of the pre-drought C stock. (c) **Conceptualized UCE-climate C change diagram:** hypothetical response in terrestrial

998 "integrated-C-change" (kg C m^{-2} yr) due to eCO$_2$ (blue line), rising temperature (red line),

999 interaction between eCO$_2$ and temperature (dashed purple), and combined interactions among

1000 eCO$_2$, temperature, and UCEs of prolonged durations (green line), all relative to a reference

1001 drought of normal duration with no warming (black line). Integrated-C-change denotes the

1002 difference in integrated-C-loss (see panel b) between a scenario of changing climatic drivers and

1003 the reference drought (control). (d) **Conceptual UCE amplification diagram**: hypothetical

1004 amplified change in forest C stocks to eCO$_2$ and temperature relative to the pre-warming

1005 historical past (based on Jump et al. (2017)). Change in C stock greater than zero indicates a

1006 'structural overshoot' (SO) due to favorable environmental conditions and/or recovery from an

1007 extreme drought-heat event (EE). Hashed black areas indicate a structural overshoot due to

1008 eCO$_2$, which occurs over the historical CO$_2$ levels (dashed blue line). Initially, an eCO$_2$ effect

1009 leads to a larger increase in structural overshoot (due to CO$_2$ fertilization), driving more extreme

1010 vegetation mortality ('mortality overshoot' - MO) relative to historical dieback events and thus a

1011 greater decrease in C stock. Increased warming through time increasingly counteracts any CO$_2$

1012 fertilization effect; while the amplitude of post-UCE C stock recoveries remains large, net C

1013 stock values eventually decline (downward curvature) due to more pronounced loss in C stocks

1014 (and greater ecosystem state change) from hotter UCEs.

1015 SO = structural overshoot, MO = mortality overshoot, EE = historically extreme drought-heat

1016 event, UCE = unprecedented climate extreme.

1017
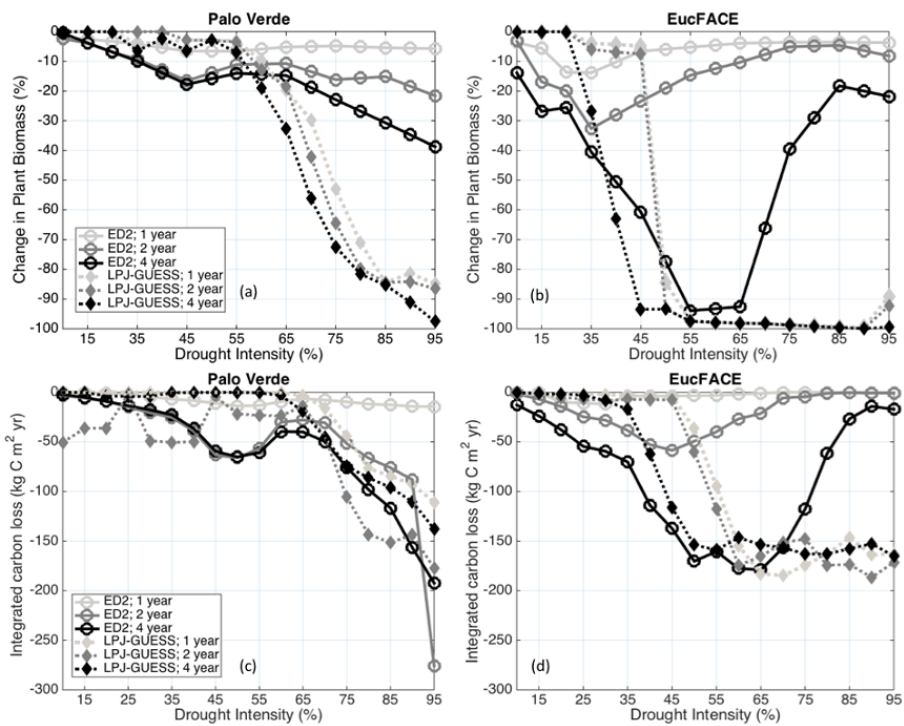
Figure 2 Modeled change in biomass (%) at the end of drought periods of different lengths (1, 2, and 4-year droughts) and intensities (up to 95% precipitation removed) at (a) Palo Verde, and (b) EucFACE, for the ED2 and LPJ-GUESS models. Modeled integrated-C-loss (C reduction due to extreme drought integrated over time until biomass recovers to 50% of the non-drought baseline biomass) at (c) Palo Verde and (d) EucFACE.

35
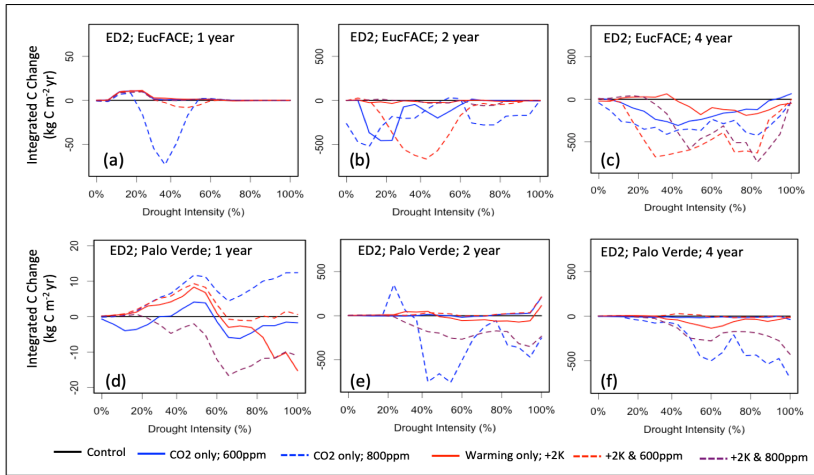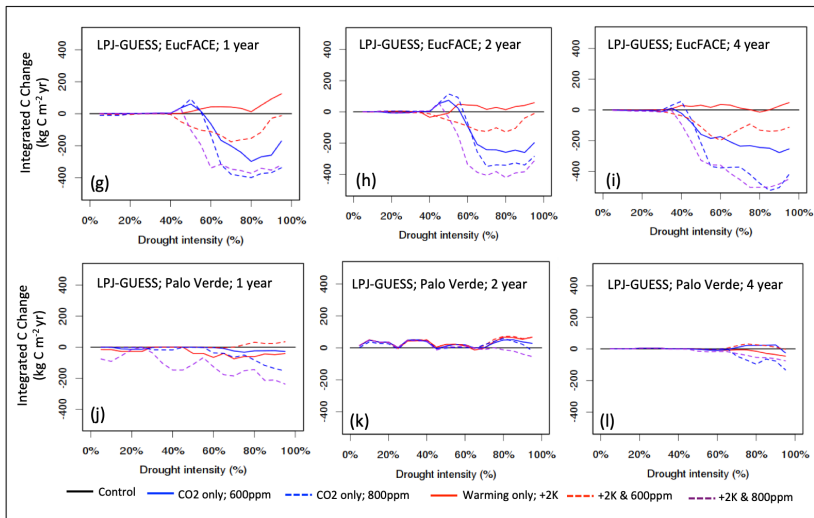
Figure 3 Vegetation C response to interactions between drought intensity (0% to 100% precipitation reduction), drought durations (1, 2, 4-year droughts), and idealized scenarios of warming and eCO_2 compared to the reference simulation, simulated by two VDMs; ED2 (a-f) and LPJ-GUESS (g-l) at two sites (EucFACE and Palo Verde). The scenarios include a control (current temperature; 400 ppm atmospheric CO_2), two eCO_2 scenarios (600 ppm or 800 ppm),

36

1032   elevated temperature (2 K above current), and a combination of eCO_2 (600 ppm or 800 ppm) and

1033   higher temperature. Vegetation response is quantified as "integrated-C-change" (in kg C m^{-2} yr;

1034   Eq. 4), which is defined as the difference in integrated-C-losses due to drought between a given

1035   scenario of change in climatic drivers and the control. Negative values for integrated-C-change

1036   indicate that warming and/or eCO_2 leads to stronger C losses and/or longer recovery, while

1037   positive values for integrated-C-change indicates a buffering effect.
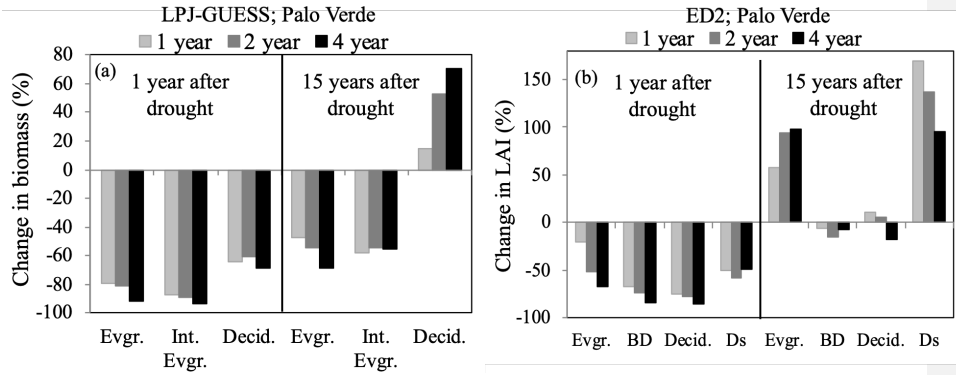
1038

1039
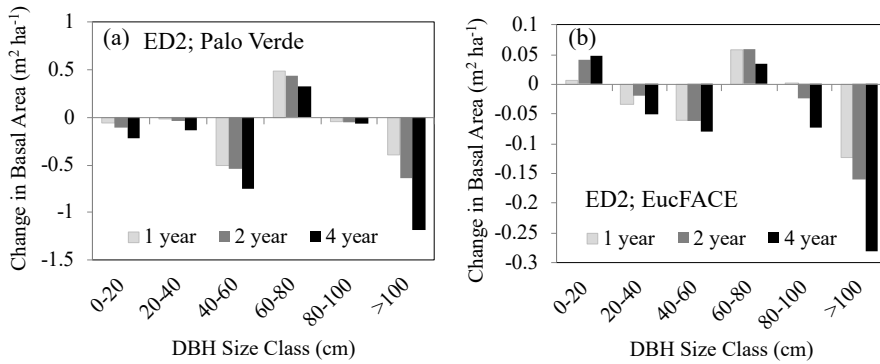
1040

1041   **Figure 4** Change in basal area (m^2 ha^{-1}) immediately following either 1, 2, or 4 year droughts for

1042   six increasing size class bins (DBH, cm) as predicted by the ED2 model for (a) the Palo Verde

1043   site, with 90% precipitation removed, and (b) the EucFACE site with 50% precipitation

1044   removed.

1045

1046
1047
1048 **Figure 5** Percent change in community composition, represented by plant functional type (PFT),

1049 the year following three drought durations of UCEs (1, 2, and 4-year droughts and 90%

1050 precipitation removed) as well as 15 years after droughts, for the tropical Palo Verde site by (a)

1051 LPJ-GUESS reported in biomass change, and (b) ED2 reported in LAI change. Even though Ds

1052 had the strongest recovery, it should be noted it was the least abundant PFT at this site. Evgr. =

1053 evergreen, Int. Ever. = intermediate evergreen, Decid. = deciduous, BD = brevi-deciduous, Ds =

1054 deciduous stem-succulent. EucFACE data not shown because only one PFT present (evergreen

1055 tree).

1056   References:

1057

1058 Adams, H.D., Guardiola-Claramonte, M., Barron-Gafford, G.A., Villegas, J.C., Breshears, D.D.,
1059   Zou, C.B. et al.: Temperature sensitivity of drought-induced tree mortality portends
1060   increased regional die-off under global-change-type drought, PNAS, 106, 7063-7066, 2009.
1061 Adams, H.D., Barron-Gafford, G.A., Minor, R.L., Gardea, A.A., Bentley, L.P., Law, D.J. et al.:
1062   Temperature response surfaces for mortality risk of tree species with future drought,
1063   Environ. Res. Lett., 12, 115014, 2017a.
1064 Adams, H.D., Zeppel, M.J.B., Anderegg, W.R.L., Hartmann, H., Landhäusser, S.M., Tissue, D.T.
1065   et al.: A multi-species synthesis of physiological mechanisms in drought-induced tree
1066   mortality, Nature Ecol. & Evol., 1, 1285-1291, 2017b.
1067 Aguirre, BA, Hsieh, B, Watson, SJ, Wright, AJ.: The experimental manipulation of atmospheric
1068   drought: Teasing out the role of microclimate in biodiversity experiments, J. Ecol., 109,
1069   1986– 1999, https://doi.org/10.1111/1365-2745.13595, 2021.
1070 Ahlström, A., Schurgers, G., Arneth, A., and Smith, B.: Robustness and uncertainty in terrestrial
1071   ecosystem carbon response to CMIP5 climate change projections, Environ. Res. Lett., 7,
1072   044008, 2012.
1073 Ainsworth, E.A., and Long, S.P.: What have we learned from 15 years of free-air CO_2
1074   enrichment (FACE)? A meta-analytic review of the responses of photosynthesis, canopy
1075   properties and plant production to rising CO_2, New Phytol., 165, 351-372, 2005.
1076 Allen, C.D., Breshears, D.D., and McDowell, N.G.: On underestimation of global vulnerability to
1077   tree mortality and forest die-off from hotter drought in the Anthropocene, Ecosphere, 6,
1078   art129, 2015.
1079 Allen, K., Dupuy, J.M., Gei, M.G., Hulshof, C.M., Medvigy, D., Pizano, C. et al.: Will seasonally
1080   dry tropical forests be sensitive or resistant to future changes in 558 rainfall regimes?
1081   Environ. Res. Lett., 12, 023001, 2017.
1082 Amiro, B.D., Barr, A.G., Barr, J.G., Black, T.A., Bracho, R., Brown, M. et al.: Ecosystem carbon
1083   dioxide fluxes after disturbance in forests of North America, J. Geophys. Res.
1084   Biogeosciences, 115, 2010.
1085 Anderegg, W.R.L., Hicke, J.A., Fisher, R.A., Allen, C.D., Aukema, J., Bentz, B. et al.: Tree
1086   mortality from drought, insects, and their interactions in a changing climate, New Phytol.,
1087   208, 674-683, 2015.
1088 Anderegg, W.R.L., Klein, T., Bartlett, M., Sack, L., Pellegrini, A.F.A., Choat, B. et al.: Meta-
1089   analysis reveals that hydraulic traits explain cross-species patterns of drought-induced tree
1090   mortality across the globe, PNAS, 113, 5024-5029, 2016a.
1091 Anderegg, W.R.L., Martinez-Vilalta, J., Cailleret, M., Camarero, J.J., Ewers, B.E., Galbraith, D.
1092   et al.: When a Tree Dies in the Forest: Scaling Climate-Driven Tree Mortality to Ecosystem
1093   Water and Carbon Fluxes, Ecosystems, 19, 1133-1147, 2016b.
1094 Anderegg, W.R.L., Konings, A.G., Trugman, A.T., Yu, K., Bowling, D.R., Gabbitas, R. et al.:
1095   Hydraulic diversity of forests regulates ecosystem resilience during drought, Nature, 561,
1096   538-541, 2018.
1097 Anderegg, W.R.L. and Venturas, M.D.: Plant hydraulics play a critical role in Earth system
1098   fluxes, New Phytol, 226, 1535-1538, https://doi.org/10.1111/nph.16548, 2020.
1099 Asner, G.P., Brodrick, P.G., Anderson, C.B., Vaughn, N., Knapp, D.E., and Martin, R.E.:
1100   Progressive forest canopy water loss during the 2012–2015 California drought. PNAS, 113,
1101   E249-E255, 2016.

39

1102 Arora, V.K., Katavouta, A., Williams, R.G., Jones, C.D., Brovkin, V., Friedlingstein, P., et al.:
1103   Carbon-concentration and carbon-climate feedbacks in CMIP6 models and their
1104   comparison to CMIP5 models, Biogeosciences, 17, 4173–4222, 2020.
1105 Bai, Y., Wu, J., Xing, Q., Pan, Q., Huang, J., Yang, D. et al.: PRIMARY PRODUCTION AND
1106   RAIN USE EFFICIENCY ACROSS A PRECIPITATION GRADIENT ON THE
1107   MONGOLIA PLATEAU, Ecology, 89, 2140-2153, 2008.
1108 Beier, C., Beierkuhnlein, C., Wohlgemuth, T., Penuelas, J., Emmett, B., Körner, C. et al.:
1109   Precipitation manipulation experiments – challenges and recommendations for the future,
1110   Ecol. Lett., 15, 899-911, 2012.
1111 Bennett, A.C., McDowell, N.G., Allen, C.D., and Anderson-Teixeira, K.J.: Larger trees suffer
1112   most during drought in forests worldwide, Nature Plants, 1, 15139, 2015.
1113 Biederman, J.A., Meixner, T., Harpold, A.A., Reed, D.E., Gutmann, E.D., Gaun, J.A. et al.:
1114   Riparian zones attenuate nitrogen loss following bark beetle-induced lodgepole pine
1115   mortality, J. Geophys. Res. Biogeosciences, 121, 933-948, 2016.
1116 Biederman, J.A., Somor, A.J., Harpold, A.A., Gutmann, E.D., Breshears, D.D., Troch, P.A. et al.:
1117   Recent tree die-off has little effect on streamflow in contrast to expected increases from
1118   historical studies, Water Resources Res., 51, 9775-9789, 2015.
1119 Blyth, E.M., Arora, V.K., Clark, D.B. et al.: Advances in Land Surface Modelling, Curr. Clim.
1120   Change Rep., 7, 45–71, https://doi.org/10.1007/s40641-021-00171-5, 2021.
1121 Borchert, R., Rivera, G., and Hagnauer, W.: Modification of Vegetative Phenology in a Tropical
1122   Semi-deciduous Forest by Abnormal Drought and Rain, Biotropica, 34, 27-39, 2002.
1123 Bonan, G.: Vegetation Demography, in: Climate Change and Terrestrial Ecosystem Modeling,
1124   Cambridge: Cambridge University Press, 344-364, doi:10.1017/9781107339217.020, 2019.
1125 Bonan, G. B., Patton, E. G., Finnigan, J. J., Baldocchi, D. D., and Harman, I. N.: Moving beyond
1126   the incorrect but useful paradigm: reevaluating big-leaf and multilayer plant canopies to
1127   model biosphere-atmosphere fluxes – a review, Agr. Forest Meteorol., 306,
1128   108435, https://doi.org/10.1016/j.agrformet.2021.108435, 2021.
1129 Brando, P.M., Paolucci, L., Ummenhofer, C.C., Ordway, E.M., Hartmann, H., Cattau, M.E.,
1130   Rattis, L., Medjibe, V., Coe, M.T., Balch, J.: Droughts, Wildfires, and Forest Carbon
1131   Cycling: A Pantropical Synthesis, Annual Review of Earth and Planetary Sciences, 47, 555-
1132   581, 2019.
1133 Breshears, D.D., Myers, O.B., Meyer, C.W., Barnes, F.J., Zou, C.B., Allen, C.D. et al.: Tree die-
1134   off in response to global change-type drought: mortality insights from a decade of plant
1135   water potential measurements, Front. Ecol. Environ., 7, 185-189, 2009.
1136 Brodribb, T.J., Bowman, D.J.M.S., Nichols, S., Delzon, S. and Burlett, R.: Xylem function and
1137   growth rate interact to determine recovery rates after exposure to extreme water deficit, New
1138   Phytol., 188, 533-542, 2010.
1139 Bugmann, H., and Seidl, R.: The evolution, complexity and diversity of models of long-term
1140   forest dynamics. J. of Ecol., 110, 2288– 2307, https://doi.org/10.1111/1365-2745.13989,
1141   2022.
1142 Carreño-Rocabado, G., Peña-Claros, M., Bongers, F., Alarcón, A., Licona, J.-C., and Poorter, L.:
1143   Effects of disturbance intensity on species and functional diversity in a tropical forest, J.
1144   Ecology, 100, 1453-1463, 2012.
1145 Chapman, T.B., Veblen, T.T., and Schoennagel, T.: Spatiotemporal patterns of mountain pine
1146   beetle activity in the southern Rocky Mountains, Ecology, 93, 2175-2185, 2012.

1147 Chiang, F., Mazdiyasni, O., and AghaKouchak, A.: Evidence of anthropogenic impacts on global
1148   drought frequency, duration, and intensity, Nat Commun., 12**,** 2754,
1149   https://doi.org/10.1038/s41467-021-22314-w, 2021.
1150 Choat, B., Brodribb, T.J., Brodersen, C.R., Duursma, R.A., López, R., and Medlyn, B.E.: Triggers
1151   of tree mortality under drought, Nature, 558, 531-539, 2018.
1152 Choat, B., Jansen, S., Brodribb, T.J., Cochard, H., Delzon, S., Bhaskar, R. et al.: Global
1153   convergence in the vulnerability of forests to drought, Nature, 491, 752-755, 2012.
1154 Christoffersen, B.O., Gloor, M., Fauset, S., Fyllas, N.M., Galbraith, D.R., Baker, T.R. et al.:
1155   Linking hydraulic traits to tropical forest function in a size-structured and trait-driven model
1156   (TFS v.1-Hydro), Geosci. Model Dev. Discuss., 2016, 1-60, 2016.
1157 Ciais, P., Reichstein, M., Viovy, N., Granier, A., Ogée, J., Allard, V. et al.: Europe-wide
1158   reduction in primary productivity caused by the heat and drought in 2003, Nature, 437, 529,
1159   2005.
1160 Ciais, P., Sabine, C., Bala, G., Bopp, L., Brovkin, V., Canadell, J., et al.: Carbon and other
1161   biogeochemical cycles. In: Climate Change 2013: The Physical Science Basis.
1162   Contribution of Working Group I to the Fifth Assessment Report of the
1163   Intergovernmental Panel on Climate Change (eds. Stocker, T.F., Qin, D., Plattner, G.-K.,
1164   Tignor, M., Allen, S.K., Boschung, J., et al.), Cambridge University Press, Cambridge,
1165   United Kingdom and New York, NY, USA, pp. 465–570, 2013.
1166 Clark, K.L., Skowronski, N., and Hom, J.: Invasive insects impact forest carbon dynamics, Glob.
1167   Change Biol., 16, 88-101, 2010.
1168 Coley, P., Massa, M., Lovelock, C., Winter, K.: Effects of elevated CO_2 on foliar chemistry of
1169   saplings of nine species of tropical tree, Oecologia, 2002.
1170 Creeden, E.P., Hicke, J.A., and Buotte, P.C.: Climate, weather, and recent mountain pine beetle
1171   outbreaks in the western United States, Forest Ecol. Manag., 312, 239-251, 2014.
1172 D'Amato, A.W., Bradford, J.B., Fraver, S. and Palik, B.J.: Effects of thinning on drought
1173   vulnerability and climate response in north temperate forest ecosystems, Eco. Applications,
1174   23, 1735-1742, 2013.
1175 da Costa, A.C.L., Galbraith, D., Almeida, S., Portela, B.T.T., da Costa, M., de Athaydes Silva
1176   Junior, J. et al., Effect of 7 yr of experimental drought on vegetation dynamics and biomass
1177   storage of an eastern Amazonian rainforest, New Phytol., 187, 579-591, 2010.
1178 De Kauwe, M.G., Medlyn, B.E., Zaehle, S., Walker, A.P., Dietze, M.C., Wang, Y.-P. et al.:
1179   Where does the carbon go? A model-data intercomparison of vegetation carbon allocation
1180   and turnover processes at two temperate forest free-air CO_2 enrichment sites, New Phytol,
1181   203, 883-899, 2014.
1182 Dietze, M.C., and Matthes, J.H.: A general ecophysiological framework for modelling the impact
1183   of pests and pathogens on forest ecosystems, Ecol. Lett., 17, 1418-1426, 2014.
1184 Döscher, R., Acosta, M., et al.: The EC-Earth3 Earth System Model for the Climate Model
1185   Intercomparison Project 6, Geosci. Model Dev. Discuss. [preprint],
1186   https://doi.org/10.5194/gmd-2020-446, in revision, 2022.
1187 Dreesen, F.E., De Boeck, H.J., Janssens, I.A., and Nijs, I: Do successive climate extremes
1188   weaken the resistance of plant communities? An experimental study using plant
1189   assemblages, Biogeosciences, 11, 109-121, 2014.
1190 Duursma, R.A., Gimeno, T.E., Boer, M.M., Crous, K.Y., Tjoelker, M.G. and Ellsworth, D.S.:
1191   Canopy leaf area of a mature evergreen *Eucalyptus* woodland does not respond to elevated

1192   atmospheric [CO_2] but tracks water availability, Glob. Change Biol., 22, 1666-
1193   1676, https://doi.org/10.1111/gcb.13151, 2016.
1194 Eamus, D., Boulain, N., Cleverly, J., and Breshears, D.D.: Global change-type drought-induced
1195   tree mortality: vapor pressure deficit is more important than temperature per se in causing
1196   decline in tree health, Ecol. Evol., 3, 2711-2729, 2013.
1197 Eller, C.B., Rowland, L., Mencuccini, M., Rosas, T., Williams, K., Harper, A. et al.: Stomatal
1198   optimization based on xylem hydraulics (SOX) improves land surface model simulation of
1199   vegetation responses to climate, New Phytol, 226, 1622-
1200   1637, https://doi.org/10.1111/nph.16419, 2020.
1201 Ellsworth, David S., Anderson, Ian C., Crous, Kristine Y., Cooke, J., Drake, John E., Gherlenda,
1202   Andrew N. et al.: Elevated CO2 does not increase eucalypt forest productivity on a low-
1203   phosphorus soil, Nature Climate Change, 7, 279, 2017.
1204 ENQUIST, B.J., and ENQUIST, C.A.F.: Long-term change within a Neotropical forest: assessing
1205   differential functional and floristic responses to disturbance and drought, Glob. Change
1206   Biol., 17, 1408-1424, 2011.
1207 Esquivel-Muelbert, A., Baker, T.R., Dexter, K.G., Lewis, S.L., Brienen, R.J.W., Feldpausch, T.R.
1208   et al.: Compositional response of Amazon forests to climate change, Glob. Change Biol., 25,
1209   39-56, 2019.
1210 Eziz, A., Yan, Z., Tian, D., Han, W., Tang, Z., and Fang, J.: Drought effect on plant biomass
1211   allocation: A meta-analysis, Ecol. Evol, 7, 11002-11010, 2017.
1212 Fang, Y., Leung, L. R., Knox, R., Koven, C., and Bond-Lamberty, B.: Impact of the numerical
1213   solution approach of a plant hydrodynamic model (v0.1) on vegetation dynamics, Geosci.
1214   Model Dev., 15, 6385–6398, https://doi.org/10.5194/gmd-15-6385-2022, 2022.
1215 Feldpausch, T.R., Phillips, O.L., Brienen, R.J.W., Gloor, E., Lloyd, J., Lopez-Gonzalez, G. et al.:
1216   Amazon forest response to repeated droughts, Global Biogeochemical Cycles, 30, 964-982,
1217   2016.
1218 Fisher, R.A., Muszala, S., Verteinstein, M., Lawrence, P., Xu, C., McDowell, N.G. et al.: Taking
1219   off the training wheels: the properties of a dynamic vegetation model without climate
1220   envelopes, CLM4.5(ED), Geosci. Model Dev., 8, 3593-3619, 2015.
1221 Fisher, R.A., Koven, C.D., Anderegg, W.R.L., Christoffersen, B.O., Dietze, M.C., Farrior, C.E. et
1222   al.: Vegetation demographics in Earth System Models: A review of progress and priorities,
1223   Glob. Change Biol., 24, 35-54, 2018.
1224 Fisher, R. A., and Koven, C. D.: Perspectives on the future of land surface models and the
1225   challenges of representing complex terrestrial systems, JAMES, 12,
1226   e2018MS001453, https://doi.org/10.1029/2018MS001453, 2020.
1227 Fleischer, K., Rammig, A., De Kauwe, M.G., Walker, A.P., Domingues, T.F., Fuchslueger, L. et
1228   al.: Amazon forest response to CO2 fertilization dependent on plant phosphorus acquisition,
1229   Nature Geoscience, 12, 736-741, 2019.
1230 Frank, D., Reichstein, M., Bahn, M., Thonicke, K., Frank, D., Mahecha, M.D. et al.: Effects of
1231   climate extremes on the terrestrial carbon cycle: concepts, processes and potential future
1232   impacts, Glob. Change Biol., 21, 2861-2880, 2015.
1233 Franklin, O., McMurtrie, R.E., Iversen, C.M., Crous, K.Y., Finzi, A.C., Tissue, D.T., Ellsworth,
1234   D.S., Oren, R. Norby, R.J.: Forest fine-root production and nitrogen use under elevated
1235 CO_2: contrasting responses in evergreen and deciduous trees explained by a common
1236   principle, Glob. Change Biol., 15, 132-144, 2009.

1237 Franklin, O., Johansson, J., Dewar, R.C., Dieckmann, U., McMurtrie, R.E., Brännström, Å.,
1238   Dybzinski, R.: Modeling carbon allocation in trees: a search for principles, Tree Physiology,
1239   32, 648–666, https://doi.org/10.1093/treephys/tpr138, 2012.
1240 Franklin, O., Harrison, S.P., Dewar, R. et al.: Organizing principles for vegetation dynamics. Nat.
1241   Plants, 6, 444–453, https://doi.org/10.1038/s41477-020-0655-x, 2020.
1242 Friend, A.D., Lucht, W., Rademacher, T.T., Keribin, R., Betts, R., Cadule, P. et al.: Carbon
1243   residence time dominates uncertainty in terrestrial vegetation responses to future climate
1244   and atmospheric CO2, PNAS, 111, 3280-3285, 2014.
1245 Gerten, D., LUO, Y., Le MAIRE, G., PARTON, W.J., KEOUGH, C., WENG, E. et al.: Modelled
1246   effects of precipitation on ecosystem carbon and water dynamics in different climatic zones,
1247   Glob. Change Biol., 14, 2365-2379, 2008.
1248 Goulden, M.L., and Bales, R.C.: California forest die-off linked to multi-year deep soil drying in
1249   2012–2015 drought, Nature Geoscience, 12, 632-637, 2019.
1250 Gray, S.B., Dermody, O., Klein, S.P., Locke, A.M., McGrath, J.M., Paul, R.E. et al.: Intensifying
1251   drought eliminates the expected benefits of elevated carbon dioxide for soybean, Nature
1252   Plants, 2, 16132, 2016.
1253 Greenwood, S., Ruiz-Benito, P., Martínez-Vilalta, J., Lloret, F., Kitzberger, T., Allen, C.D. et al.:
1254   Tree mortality across biomes is promoted by drought intensity, lower wood density and
1255   higher specific leaf area, Ecol. Lett., 20, 539-553, 2017.
1256 Griffin, D., and Anchukaitis, K.J.: How unusual is the 2012–2014 California drought? Geophys.
1257   Res. Lett., 41, 9017-9023, 2014.
1258 Hanbury-Brown, A.R., Powell, T.L., Muller-Landau, H.C., Wright, S.J. and Kueppers, L.M.:
1259   Simulating environmentally-sensitive tree recruitment in vegetation demographic models,
1260   New Phytol., 235, 78-93, https://doi.org/10.1111/nph.18059, 2022.
1261 Harrison, S.P., Cramer, W., Franklin, O., Prentice, I.C., Wang, H., Brännström, Å., et al.: Eco-
1262   evolutionary optimality as a means to improve vegetation and land-surface models, New
1263   Phytol., 231, 2125-2141, https://doi.org/10.1111/nph.17558, 2021.
1264 Hickler, T., Smith, B., Sykes, M.T., Davis, M.B., Sugita, S., and Walker, K.: USING A
1265   GENERALIZED VEGETATION MODEL TO SIMULATE VEGETATION DYNAMICS
1266   IN NORTHEASTERN USA, Ecology, 85, 519-530, 2004.
1267 Holm, J. A., Knox, R. G., Zhu, Q., Fisher, R. A., Koven, C. D., Nogueira Lima, A. J., et al.: The
1268   central Amazon biomass sink under current and future atmospheric CO_2: Predictions from
1269   big-leaf and demographic vegetation models, J. Geophys. Res. Biogeosciences, 125,
1270   e2019JG005500. https://doi.org/10.1029/2019JG005500, 2020.
1271 Hovenden, M.J., Newton, P.C.D., and Wills, K.E.: Seasonal not annual rainfall determines
1272   grassland biomass response to carbon dioxide, Nature, 511, 583, 2014.
1273 Hubbard, R.M., Rhoades, C.C., Elder, K., and Negron, J.: Changes in transpiration and foliage
1274   growth in lodgepole pine trees following mountain pine beetle attack and mechanical
1275   girdling, Forest Ecol. Manag., 289, 312-317, 2013.
1276 IPCC: Managing the Risks of Extreme Events and Disasters to Advance Climate Change
1277   Adaptation. A Special Report of Working Groups I and II of the Intergovernmental Panel on
1278   Climate Change. (ed. Field, C.B., V. Barros, T.F. Stocker, D. Qin, D.J. Dokken, K.L. Ebi,
1279   M.D. Mastrandrea, K.J. Mach, G.-K. Plattner, S.K. Allen, M. Tignor, and P.M. Midgley)
1280   Cambridge, UK, and New York, NY, USA, p. 582 pp, 2012.
1281 IPCC: Climate Change 2021: The Physical Science Basis. Contribution of Working Group I to the
1282   Sixth Assessment Report of the Intergovernmental Panel on Climate Change [Masson-

1283   Delmotte, V., P. Zhai, A. Pirani, S.L. Connors, C. Péan, S. Berger, N. Caud, Y. Chen, L.
1284   Goldfarb, M.I. Gomis, M. Huang, K. Leitzell, E. Lonnoy, J.B.R. Matthews, T.K. Maycock,
1285   T. Waterfield, O. Yelekçi, R. Yu, and B. Zhou (eds.)]. Cambridge University Press, 2021.
1286   Jiang, M., Medlyn, B.E., Drake, J.E., Duursma, R.A., Anderson, I.C., Barton, C.V.M., Boer,
1287   M.B., Carrillo, Y., Castañeda-Gómez, L., Collins, L., et al.: The fate of carbon in a mature
1288   forest under carbon dioxide enrichment, Nature, 580, 227-231,
1289   https://doi.org/10.1038/s41586-020-2128-9, 2020.
1290   Joslin, J.D., Wolfe, M.H., and Hanson, P.J.: Effects of altered water regimes on forest root
1291   systems, New Phytol., 147, 117-129, 2000.
1292   Jump, A.S., Ruiz-Benito, P., Greenwood, S., Allen, C.D., Kitzberger, T., Fensham, R. et al.:
1293   Structural overshoot of tree growth with climate variability and the global spectrum of
1294   drought-induced forest dieback, Glob. Change Biol., 23, 3742-3757, 2017.
1295   Kalacska, M.E.R., Sánchez-Azofeifa, G.A., Calvo-Alvarado, J.C., Rivard, B. and Quesada, M.:
1296   Effects of Season and Successional Stage on Leaf Area Index and Spectral Vegetation
1297   Indices in Three Mesoamerican Tropical Dry Forests, Biotropica, 37, 486-
1298   496, https://doi.org/10.1111/j.1744-7429.2005.00067.x, 2005.
1299   Kannenberg, S.A., Schwalm, C.R. and Anderegg, W.R.L.: Ghosts of the past: how drought legacy
1300   effects shape forest functioning and carbon cycling, Ecol. Lett., 23: 891-901,
1301   https://doi.org/10.1111/ele.13485, 2020.
1302   Kattge, J., DÍAZ, S., LAVOREL, S., PRENTICE, I.C., LEADLEY, P., BÖNISCH, G. et al.: TRY
1303   – a global database of plant traits, Global Change Biol, 17, 2905-2935, 2011.
1304   Kayler, Z.E., De Boeck, H.J., Fatichi, S., Grünzweig, J.M., Merbold, L., Beier, C. et al.:
1305   Experiments to confront the environmental extremes of climate change, Front. Ecol.
1306   Environ., 13, 219-225, 2015.
1307   Keenan, T.F., Hollinger, D.Y., Bohrer, G., Dragoni, D., Munger, J.W., Schmid, H.P. et al.:
1308   Increase in forest water-use efficiency as atmospheric carbon dioxide concentrations rise,
1309   Nature, 499, 324-327, 2013.
1310   Kennedy, D., Swenson, S., Oleson, K. W., Lawrence, D. M., Fisher, R., Lola da Costa, A. C., and
1311   Gentine, P.: Implementing plant hydraulics in the Community Land Model, version 5,
1312   JAMES, 11, 485– 513, https://doi.org/10.1029/2018MS001500, 2019.
1313   Li, L., Yang, Z.-L., Matheny, A. M., Zheng, H., Swenson, S. C., Lawrence, D. M., et
1314   al.: Representation of plant hydraulics in the Noah-MP land surface model: Model
1315   development and multiscale evaluation, JAMES, 13,
1316   e2020MS002214, https://doi.org/10.1029/2020MS002214, 2021.
1317   Li, Q., Lu, X., Wang, Y., Huang, X., Cox, P. M., and Luo, Y.: Leaf area index identified as a
1318   major source of variability in modeled CO_2 fertilization, Biogeosciences, 15, 6909–6925,
1319   https://doi.org/10.5194/bg-15-6909-2018, 2018.
1320   Liu, Y., Parolari, A.J., Kumar, M., Huang, C.-W., Katul, G.G., and Porporato, A.: Increasing
1321   atmospheric humidity and CO2 concentration alleviate forest mortality risk, PNAS, 114,
1322   9918-9923, 2017.
1323   Lloret, F., Escudero, A., Iriondo, J.M., Martínez-Vilalta, J., and Valladares, F.: Extreme climatic
1324   events and vegetation: the role of stabilizing processes, Glob. Change Biol., 18, 797-805,
1325   2012.
1326   Luo, Y., Gerten, D., Le Maire, G., Parton, W.J., Weng, E., Zhou, X. et al.: Modeled interactive
1327   effects of precipitation, temperature, and [CO2] on ecosystem carbon and water dynamics in
1328   different climatic zones, Glob. Change Biol., 14, 1986-1999, 2008.

44

Luo, Y.Q., Randerson, J.T., Abramowitz, G., Bacour, C., Blyth, E., Carvalhais, N. et al.: A framework for benchmarking land models, Biogeosciences, 9, 3857-3874, 2012.

Luo, Y., Jiang, L., Niu, S., Zhou, X.: Nonlinear responses of land ecosystems to variation in precipitation, New Phytol., 214, 5–7, 2017.

Ma, W., Zhai, L., Pivovaroff, A., Shuman, J., Buotte, P., Ding, J., Christoffersen, B., Knox, R., Moritz, M., Fisher, R. A., Koven, C. D., Kueppers, L., and Xu, C.: Assessing climate change impacts on live fuel moisture and wildfire risk using a hydrodynamic vegetation model, Biogeosciences, 18, 4005–4020, https://doi.org/10.5194/bg-18-4005-2021, 2021.

MacGillivray, C.W., Grime, J.P., and The Integrated Screening Programme, T.: Testing Predictions of the Resistance and Resilience of Vegetation Subjected to Extreme Events, Funct. Ecol., 9, 640-649, 1995.

Markewitz, D., Devine, S., Davidson, E.A., Brando, P., and Nepstad, D.C.: Soil moisture depletion under simulated drought in the Amazon: impacts on deep root uptake, New Phytol., 187, 592-607, 2010.

Matusick, G., Ruthrof, K.X., Brouwers, N.C., Dell, B., and Hardy, G.S.J.: Sudden forest canopy collapse corresponding with extreme drought and heat in a mediterranean-type eucalypt forest in southwestern Australia, European J. Forest Res., 132, 497-510, 2013.

Matusick, G., Ruthrof, K.X., Fontaine, J.B., and Hardy, G.E.S.J.: Eucalyptus forest shows low structural resistance and resilience to climate change-type drought, J. Vegetation Science, 27, 493-503, 2016.

McCarthy, M.C., and Enquist, B.J.: Consistency between an allometric approach and optimal partitioning theory in global patterns of plant biomass allocation, Funct. Ecol., 21, 713-720, 2007.

McDowell, N., Pockman, W.T., Allen, C.D., Breshears, D.D., Cobb, N., Kolb, T. et al.: Mechanisms of plant survival and mortality during drought: why do some plants survive while others succumb to drought? New Phytol., 178, 719-739, 2008.

McDowell, N.G., Adams, H.D., Bailey, J.D., Hess, M., and Kolb, T.E.: Homeostatic Maintenance Of Ponderosa Pine Gas Exchange In Response To Stand Density Changes, Ecological Applications, 16, 1164-1182, 2006.

McDowell, N.G., and Allen, C.D.: Darcy's law predicts widespread forest mortality under climate warming, Nature Climate Change, 5, 669-672, 2015.

McDowell, N.G., Beerling, D.J., Breshears, D.D., Fisher, R.A., Raffa, K.F., and Stitt, M.: The interdependence of mechanisms underlying climate-driven vegetation mortality, Trends in Ecol. & Evolution, 26, 523-532, 2011.

McDowell, N.G., Fisher, R.A., Xu, C., Domec, J.C., Hölttä, T., Mackay, D.S. et al.: Evaluating theories of drought-induced vegetation mortality using a multimodel–experiment framework, New Phytol., 200, 304-321, 2013.

Medlyn, B.E., De Kauwe, M.G., Zaehle, S., Walker, A.P., Duursma, R.A., Luus, K., Mishurov, M., Pak, B., Smith, B., Wang, Y.-P., Yang, X., Crous, K.Y., Drake, J.E., Gimeno, T.E., Macdonald, C.A., Norby, R.J., Power, S.A., Tjoelker, M.G. and Ellsworth, D.S.: Using models to guide field experiments: a priori predictions for the CO2 response of a nutrient- and water-limited native Eucalypt woodland, Glob. Change Biol., 22, 2834-2851, 2016.

Medvigy, D., Wang, G., Zhu, Q., Riley, W.J., Trierweiler, A.M., Waring, B., Xu, X. and Powers, J.S.: Observed variation in soil properties can drive large variation in modelled forest functioning and composition during tropical forest secondary succession, New Phytol, 223, 1820-1833, https://doi.org/10.1111/nph.15848, 2019.

Medvigy, D., Clark, K.L., Skowronski, N.S., and Schäfer, K.V.R.: Simulated impacts of insect defoliation on forest carbon dynamics, Environ. Res. Lett., 7, 045703, 2012.

Medvigy, D. and Moorcroft, P.R.: Predicting ecosystem dynamics at regional scales: an evaluation of a terrestrial biosphere model for the forests of northeastern North America, Philosophical Transactions of the Royal Society B: Biological Sciences, 367, 222-235, 2012.

Medvigy, D., Wofsy, S., Munger, J., Hollinger, D. and Moorcroft, P.: Mechanistic scaling of ecosystem function and dynamics in space and time: Ecosystem Demography model version 2, J. Geophys. Res. Biogeosciences, 114, 2009.

Mencuccini, M., Manzoni, S., and Christoffersen, B.: Modelling water fluxes in plants: from tissues to biosphere, New Phytol., 222, 1207-1222, https://doi.org/10.1111/nph.15681, 2019.

Meir, P., Wood, T.E., Galbraith, D.R., Brando, P.M., Da Costa, A.C.L., Rowland, L. et al.: Threshold Responses to Soil Moisture Deficit by Trees and Soil in Tropical Rain Forests: Insights from Field Experiments, BioScience, 65, 882-892, 2015.

Montané, F., Fox, A.M., Arellano, A.F., MacBean, N., Alexander, M.R., Dye, A. et al.: Evaluating the effect of alternative carbon allocation schemes in a land surface model (CLM4.5) on carbon fluxes, pools, and turnover in temperate forests, Geosci. Model Dev., 10, 3499-3517, 2017.

Muldavin, E.H., Moore, D.I., Collins, S.L., Wetherill, K.R., and Lightfoot, D.C.: Aboveground net primary production dynamics in a northern Chihuahuan Desert ecosystem, Oecologia, 155, 123-132, 2008.

Myers, J.A., and Kitajima, K.: Carbohydrate storage enhances seedling shade and stress tolerance in a neotropical forest, J. Ecology, 95, 383-395, 2007.

Niklas, K. J.: The scaling of plant height: A comparison among major plant clades and anatomical grades, Annals of Botany, 72, 165–172, https://doi.org/10.1006/anbo.1993.1095, 1993.

Norby, R.J., DeLucia, E.H., Gielen, B., Calfapietra, C., Giardina, C.P., King, J.S. et al.: Forest response to elevated CO2 is conserved across a broad range of productivity, PNAS, 102, 18052-18056, 2005.

O'Brien, M.J., Leuzinger, S., Philipson, C.D., Tay, J., and Hector, A.: Drought survival of tropical tree seedlings enhanced by non-structural carbohydrate levels, Nature Climate Change, 4, 710, 2014.

Obermeier, W.A., Lehnert, L.W., Kammann, C.I., Müller, C., Grünhage, L., Luterbacher, J. et al.: Reduced CO2 fertilization effect in temperate C3 grasslands under more extreme weather conditions, Nature Climate Change, 7, 137, 2016.

Palace, M., Keller, M., and Silva, H.: NECROMASS PRODUCTION: STUDIES IN UNDISTURBED AND LOGGED AMAZON FORESTS, Ecological Applications, 18, 873-884, 2008.

Petit, G., Anfodillo, T., Mencuccini, M.: Tapering of xylem conduits and hydraulic limitations in sycamore (*Acer pseudoplatanus*) trees, New Phytol., 177, 653-664. https://doi.org/10.1111/j.1469-8137.2007.02291.x, 2008.

Phillips, O.L., Aragão, L.E.O.C., Lewis, S.L., Fisher, J.B., Lloyd, J., López-González, G. et al.: Drought Sensitivity of the Amazon Rainforest, Science, 323, 1344-1347, 2009.

Phillips, O.L., van der Heijden, G., Lewis, S.L., López-González, G., Aragão, L.E.O.C., Lloyd, J. et al.: Drought–mortality relationships for tropical forests, New Phytol., 187, 631-646, 2010.

Pilon, C.E., Côté, B., and Fyles, J.W.: Effect of an artificially induced drought on leaf peroxidase activity, mineral nutrition and growth of sugar maple, Plant and Soil, 179, 151-158, 1996.

1421 Potter, C., Klooster, S., Hiatt, C., Genovese, V., and Castilla-Rubio, J.C.: Changes in the carbon
1422   cycle of Amazon ecosystems during the 2010 drought, Environ. Res. Lett., 6, 034024, 2011.
1423 Powell, T.L., Galbraith, D.R., Christoffersen, B.O., Harper, A., Imbuzeiro, H.M.A., Rowland, L.
1424   et al.: Confronting model predictions of carbon fluxes with measurements of Amazon
1425   forests subjected to experimental drought, New Phytol., 200, 350-365, 2013.
1426 Powell, T.L., Koven, C.D., Johnson, D.J., Faybishenko, B., Fisher, R.A., Knox, Ryan G. et al.:
1427   Variation in hydroclimate sustains tropical forest biomass and promotes functional diversity,
1428   New Phytol., 219, 932-946, 2018.
1429 Powers, J.S., Becknell, J.M., Irving, J., and Pèrez-Aviles, D.: Diversity and structure of
1430   regenerating tropical dry forests in Costa Rica: Geographic patterns and environmental
1431   drivers, Forest Ecol. Manag., 258, 959-970, 2009.
1432 Powers, J.S., and Peréz-Aviles, D.: Edaphic Factors are a More Important Control on Surface
1433   Fine Roots than Stand Age in Secondary Tropical Dry Forests, Biotropica, 45, 1-9, 2013.
1434 Powers, JS, Vargas G., G, Brodribb, TJ, et al.: A catastrophic tropical drought kills hydraulically
1435   vulnerable tree species, Glob. Change Biol. 2020; 26: 3122– 3133,
1436   https://doi.org/10.1111/gcb.15037, 2020.
1437 Pugh, T.A.M., Rademacher, T., Shafer, S. L., Steinkamp, J., Barichivich, J., Beckage, B. et al.:
1438   Understanding the uncertainty in global forest carbon turnover, Biogeosciences, 17, 3961–
1439   3989, https://doi.org/10.5194/bg-17-3961-2020, 2020.
1440 Rapparini, F., and Peñuelas, J.: Mycorrhizal Fungi to Alleviate Drought Stress on Plant Growth.
1441   In: Use of Microbes for the Alleviation of Soil Stresses, Volume 1 (ed. Miransari, M),
1442   Springer New York New York, NY, pp. 21-42, 2014.
1443 Reich, P.B., Hobbie, S.E., and Lee, T.D.: Plant growth enhancement by elevated CO_2 eliminated
1444   by joint water and nitrogen limitation, Nature Geoscience, 7, 920, 2014.
1445 Reich, P.B., Wright, I.J., and Lusk, C.H.: PREDICTING LEAF PHYSIOLOGY FROM SIMPLE
1446   PLANT AND CLIMATE ATTRIBUTES: A GLOBAL GLOPNET ANALYSIS, Ecological
1447   Applications, 17, 1982-1988, 2007.
1448 Reichstein, M., Bahn, M., Ciais, P., Frank, D., Mahecha, M.D., Seneviratne, S.I. et al.: Climate
1449   extremes and the carbon cycle, Nature, 500, 287-295, 2013.
1450 Reyes, J.J., Tague, C.L., Evans, R.D., and Adam, J.C.: Assessing the Impact of Parameter
1451   Uncertainty on Modeling Grass Biomass Using a Hybrid Carbon Allocation Strategy, 9,
1452   2968-2992, 2017.
1453 Richardson, A.D., Carbone, M.S., Keenan, T.F., Czimczik, C.I., Hollinger, D.Y., Murakami, P. et
1454   al.: Seasonal dynamics and age of stemwood nonstructural carbohydrates in temperate forest
1455   trees, New Phytol., 197, 850-861, 2013.
1456 Rowland, L., da Costa, A.C.L., Galbraith, D.R., Oliveira, R.S., Binks, O.J., Oliveira, A.A.R. et
1457   al.: Death from drought in tropical forests is triggered by hydraulics not carbon starvation,
1458   Nature, 528, 119, 2015.
1459 Roy, J., Picon-Cochard, C., Augusti, A., Benot, M.-L., Thiery, L., Darsonville, O. et al.: Elevated
1460 CO_2 maintains grassland net carbon uptake under a future heat and drought extreme, PNAS,
1461   113, 6224-6229, 2016.
1462 Ruppert, J.C., Harmoney, K., Henkin, Z., Snyman, H.A., Sternberg, M., Willms, W. et al.:
1463   Quantifying drylands' drought resistance and recovery: the importance of drought intensity,
1464   dominant life history and grazing regime, Glob. Change Biol., 21, 1258-1270, 2015.
1465 Rustad, L.E.: The response of terrestrial ecosystems to global climate change: Towards an
1466   integrated approach, Science of The Total Environ., 404, 222-235, 2008.

1467 Ruthrof, K.X., Breshears, D.D., Fontaine, J.B., Froend, R.H., Matusick, G., Kala, J. et al.:
1468   Subcontinental heat wave triggers terrestrial and marine, multi-taxa responses, Scientific
1469   Reports, 8, 13094, 2018.
1470 Scheiter, S., Langan, L., and Higgins, S.I.: Next-generation dynamic global vegetation models:
1471   learning from community ecology, New Phytol., 198, 957-969, 2013.
1472 Schenk, H.J., and Jackson, R.B.: Mapping the global distribution of deep roots in relation to
1473   climate and soil characteristics, Geoderma, 126, 129-140, 2005.
1474 Schwalm, C.R., Anderegg, W.R.L., Michalak, A.M., Fisher, J.B., Biondi, F., Koch, G. et al.:
1475   Global patterns of drought recovery, Nature, 548, 202, 2017.
1476 Seneviratne, S.I., X. Zhang, M. Adnan, W. Badi, C. Dereczynski, A. Di Luca, S. Ghosh, I.
1477   Iskandar, J. Kossin, S. Lewis, F. Otto, I. Pinto, M. Satoh, S.M. Vicente-Serrano, M. Wehner,
1478   and B. Zhou, 2021: Weather and Climate Extreme Events in a Changing Climate. In
1479   Climate Change 2021: The Physical Science Basis. Contribution of Working Group I to the
1480   Sixth Assessment Report of the Intergovernmental Panel on Climate Change [Masson-
1481   Delmotte, V., P. Zhai, A. Pirani, S.L. Connors, C. Péan, S. Berger, N. Caud, Y. Chen, L.
1482   Goldfarb, M.I. Gomis, M. Huang, K. Leitzell, E. Lonnoy, J.B.R. Matthews, T.K. Maycock,
1483   T. Waterfield, O. Yelekçi, R. Yu, and B. Zhou (eds.)], Cambridge University Press,
1484   Cambridge, United Kingdom and New York, NY, USA, pp. 1513–1766,
1485   doi:10.1017/9781009157896.013, 2021.
1486 Settele, J., Scholes, R., Betts, R., Bunn, S.E., Leadley, P., Nepstad, D., Overpeck, J.T., and
1487   Taboada, M.A.: Terrestrial and inland water systems. In: Climate Change 2014: Impacts,
1488   Adaptation, and Vulnerability. Part A: Global and Sectoral Aspects. Contribution of
1489   Working Group II to the Fifth Assessment Report of the Intergovernmental Panel on
1490   Climate Change, Cambridge University Press Cambridge, United Kingdom and New York,
1491   NY, USA, pp. 271-359, 2014.
1492 Sheffield, J., Goteti, G., and Wood, E.F.: Development of a 50-Year High-Resolution Global
1493   Dataset of Meteorological Forcings for Land Surface Modeling, J. Climate, 19, 3088-3111,
1494   2006.
1495 Shiels, A.B., Zimmerman, J.K., García-Montiel, D.C., Jonckheere, I., Holm, J., Horton, D. et al.:
1496   Plant responses to simulated hurricane impacts in a subtropical wet forest, Puerto Rico, J.
1497   Ecology, 98, 659-673, 2010.
1498 Silva, M., Matheny, A. M., Pauwels, V. R. N., Triadis, D., Missik, J. E., Bohrer, G., and Daly, E.:
1499   Tree hydrodynamic modelling of the soil–plant–atmosphere continuum using FETCH3,
1500   Geosci. Model Dev., 15, 2619–2634, https://doi.org/10.5194/gmd-15-2619-2022, 2022.
1501 Sippel, S., Zscheischler, J., and Reichstein, M.: Ecosystem impacts of climate extremes crucially
1502   depend on the timing, PNAS, 113, 5768-5770, 2016.
1503 Sitch, S., HUNTINGFORD, C., GEDNEY, N., LEVY, P.E., LOMAS, M., PIAO, S.L. et al.:
1504   Evaluation of the terrestrial carbon cycle, future plant geography and climate-carbon cycle
1505   feedbacks using five Dynamic Global Vegetation Models (DGVMs), Glob. Change Biol.,
1506   14, 2015-2039, 2008.
1507 Skelton, R.P., West, A.G., and Dawson, T.E.: Predicting plant vulnerability to drought in
1508   biodiverse regions using functional traits, PNAS, 112, 5744-5749, 2015.
1509 Smith, B., Prentice, I.C., and Sykes, M.T.: Representation of vegetation dynamics in the
1510   modelling of terrestrial ecosystems: comparing two contrasting approaches within European
1511   climate space, Global Ecol. Biogeo., 10, 621-637, 2001.

Smith, B., Wårlind, D., Arneth, A., Hickler, T., Leadley, P., Siltberg, J. et al.: Implications of incorporating N cycling and N limitations on primary production in an individual-based dynamic vegetation model, Biogeosciences, 11, 2027-2054, 2014.

Spasojevic, M.J., Bahlai, C.A., Bradley, B.A., Butterfield, B.J., Tuanmu, M.-N., Sistla, S. et al.: Scaling up the diversity–resilience relationship with trait databases and remote sensing data: the recovery of productivity after wildfire, Glob. Change Biol., 22, 1421-1432, 2016.

Sperry, J.S., Hacke, U.G., Oren, R., and Comstock, J.P.: Water deficits and hydraulic limits to leaf water supply, Plant, Cell & Environ., 25, 251-263, 2002.

Sperry, J.S., and Love, D.M.: What plant hydraulics can tell us about responses to climate-change droughts, New Phytol., 207, 14-27, 2015.

Sperry, J.S., Wang, Y., Wolfe, B.T., Mackay, D.S., Anderegg, W.R.L., McDowell, N.G. et al.: Pragmatic hydraulic theory predicts stomatal responses to climatic water deficits, New Phytol., 212, 577-589, 2016.

Stovall, A.E.L., Shugart, H., and Yang, X.: Tree height explains mortality risk during an intense drought, Nature Communications, 10, 4385, 2019.

Tague, C.L., and Moritz, M.A.: Plant Accessible Water Storage Capacity and Tree-Scale Root Interactions Determine How Forest Density Reductions Alter Forest Water Use and Productivity, Front. Forests and Global Change, 2, 2019.

Tomasella M, Petrussa E, Petruzzellis F, Nardini A, Casolo V.: The Possible Role of Non-Structural Carbohydrates in the Regulation of Tree Hydraulics, International Journal of Molecular Sciences, 21:144, https://doi.org/10.3390/ijms21010144, 2020.

Trugman, A.T., Detto, M., Bartlett, M.K., Medvigy, D., Anderegg, W.R.L., Schwalm, C. et al.: Tree carbon allocation explains forest drought-kill and recovery patterns, Ecol. Lett., 21, 1552-1560, 2018.

Trugman, A.T., Anderegg, L.D.L., Sperry, J.S., Wang, Y., Venturas, M., Anderegg, W.R.L.: Leveraging plant hydraulics to yield predictive and dynamic plant leaf allocation in vegetation models with climate change, Glob. Change Biol., 25, 4008– 4021. https://doi.org/10.1111/gcb.14814, 2019.

Uriarte, M., Lasky, J.R., Boukili, V.K., and Chazdon, R.L.: A trait-mediated, neighbourhood approach to quantify climate impacts on successional dynamics of tropical rainforests, Funct. Ecol., 30, 157-167, 2016.

Vargas G., G., Brodribb, T.J., Dupuy, J.M., González-M., R., Hulshof, C.M., Medvigy, D., Allerton, T.A.P., Pizano, C., Salgado-Negret, B., Schwartz, N.B., Van Bloem, S.J., Waring, B.G. and Powers, J.S.: Beyond leaf habit: generalities in plant function across 97 tropical dry forest tree species, New Phytol., 232: 148-161. https://doi.org/10.1111/nph.17584, 2021.

Venturas, M. D., Todd, H. N., Trugman, A. T., and Anderegg, W. R.: Understanding and predicting forest mortality in the western United States using long-term forest inventory data and modeled hydraulic damage, New Phytol., 230, 1896-1910, 2021.

Wang, D., Heckathorn, S.A., Wang, X., and Philpott, S.M.: A meta-analysis of plant physiological and growth responses to temperature and elevated CO2, Oecologia, 169, 1-13, 2012.

Weng, E.S., Malyshev, S., Lichstein, J.W., Farrior, C.E., Dybzinski, R., Zhang, T. et al.: Scaling from individual trees to forests in an Earth system modeling framework using a mathematically tractable model of height-structured competition, Biogeosciences, 12, 2655-2694, 2015.

1557 Williams, A.P., Allen, C.D., Macalady, A.K., Griffin, D., Woodhouse, C.A., Meko, D.M. et al.:
1558   Temperature as a potent driver of regional forest drought stress and tree mortality, Nature
1559   Climate Change, 3, 292, 2012.
1560 Williams, A.P., Seager, R., Berkelhammer, M., Macalady, A.K., Crimmins, M.A., Swetnam,
1561   T.W. et al.: Causes and Implications of Extreme Atmospheric Moisture Demand during the
1562   Record-Breaking 2011 Wildfire Season in the Southwestern United States, J. Applied
1563   Meteorology and Climatology, 53, 2671-2684, 2014.
1564 Williams, L.J., Bunyavejchewin, S., and Baker, P.J.: Deciduousness in a seasonal tropical forest
1565   in western Thailand: interannual and intraspecific variation in timing, duration and
1566   environmental cues, Oecologia, 155, 571-582, 2008.
1567 Wullschleger, S.D., Hanson, P.J., and Todd, D.E.: Transpiration from a multi-species deciduous
1568   forest as estimated by xylem sap flow techniques, For. Ecol. and Manage., 143, 205-213,
1569   2001.
1570 Xu, X., Medvigy, D., Powers, J.S., Becknell, J.M. and Guan, K.: Diversity in plant hydraulic
1571   traits explains seasonal and inter-annual variations of vegetation dynamics in seasonally dry
1572   tropical forests, New Phytol., 212, 80-95, 2016.
1573 Yang, Y., Hillebrand, H., Lagisz, M., Cleasby, I., and Nakagawa, S.: Low statistical power and
1574   overestimated anthropogenic impacts, exacerbated by publication bias, dominate field
1575   studies in global change biology. Glob. Change Biol., 28, 969– 989,
1576   https://doi.org/10.1111/gcb.15972, 2022.
1577 Zhu, K., Chiariello, N.R., Tobeck, T., Fukami, T., and Field, C.B.: Nonlinear, interacting
1578   responses to climate limit grassland production under global change, PNAS, 113, 10589-
1579   10594, 2016.
1580 Zhu, S-D., Chen, Y-J., Ye, Q., He, P-C., Liu, H., and Li, R-H., et al.: Leaf turgor loss point is
1581   correlated with drought tolerance and leaf carbon economics traits, Tree Physiol., 38, 658–
1582   663, https://doi.org/10.1093/treephys/tpy013, 2018.
1583 Zscheischler, J., Mahecha, M.D., von Buttlar, J., Harmeling, S., Jung, M., Rammig, A. et al.: A
1584   few extreme events dominate global interannual variability in gross primary production,
1585   Environ. Res. Lett., 9, 035001, 2014.
1586

Deleted: Zhu, Q., Riley, W.J., Tang, J., Collier, N., Hoffman, F.M., Yang, X. et al.: Representing Nitrogen, Phosphorus, and Carbon Interactions in the E3SM Land Model: Development and Global Benchmarking, 11, 2238-2258, 2019. ¶

1592
1593 **Supplemental Material:**
1594
1595 **Exploring the impacts of unprecedented climate extremes on forest ecosystems: hypotheses**
1596 **to guide modeling and experimental studies**
1597
1598 Jennifer A. Holm, David M. Medvigy, Benjamin Smith, Jeffrey S. Dukes, Claus Beier, Mikhail
1599 Mishurov, Xiangtao Xu, Jeremy W. Lichstein, Craig D. Allen, Klaus S. Larsen, Yiqi Luo, Cari
1600 Ficken, William T. Pockman, William R.L. Anderegg, and Anja Rammig
1601
1602 **Supplement Figures:**
1603
1604 **Table S1.** Terrestrial model full name, select characteristics, and associated references for the
1605 models listed throughout the manuscript.
1606

Model	Full Name	Type & Canopy	Dynamic Vegetation?	Plant Hydraulics?	References
CABLE	Community Atmosphere-Biosphere-Land Exchange	Big leaf; Single layer	No	No	Wang et al., (2011);
CABLE-POP	Community Atmosphere-Biosphere-Land Exchange - Population Orders Physiology	Cohort; Single layer	No	No	Haverd et al., (2018)
CLM5	Community Land Model v5	Big leaf; Single layer	No	Yes	Lawrence et al., (2019)
ED2-hydro	Ecosystem Demography v.2 - Hydro	Cohort; Multi-layer	Yes	Yes	Xu et al., (2016); Xu et al., (2021)
FATES	Functionally Assembled Terrestrial Ecosystem Simulator	Cohort; Multi-layer	Yes	No	Fisher et al., (2015)
FATES-HYDRO	Functionally Assembled Terrestrial Ecosystem Simulator - Hydro	Cohort; Multi-layer	Yes	Yes	Fang et al., (2022)
JSBACH4.0	JSBACH v4 DGVM	Patch-tiling; Single layer	No	No	Nabel et al., (2020)

JULES	Joint UK Land Environment Simulator	Big leaf; Single layer	No	Yes	Eller et al., (2020)
LM3-PPA	Land Model v3 – Perfect Plasticity Approximation	Cohort; Multi-layer	Yes	No	Weng et al., (2015)
LPJ-GUESS	Lund-Potsdam-Jena General Ecosystem Simulator	Cohort; Multi-layer	Yes	No	Smith et al., (2001); Smith et al., (2014)
Noah-MP-PHS	Noah-Multiparameterization - Plant Hydraulics Scheme	Big leaf; Single layer	No	Yes	Li et al., (2021)
ORCHIDEE	ORganizing Carbon and Hydrology in Dynamic EcosystEms	Big leaf; Single layer	Yes	No	Krinner et al., (2005); Druel et al., (2019)
SEIB-DGVM	Spatially Explicit Individual-Based Dynamic Global Vegetation Model	Individual; Multi-layer	Yes	No	Sato et al., (2007)
TFSv.1-Hydro	Trait Forest Simulator v1 - Hyrdo	Individual; Multi-layer	No	Yes	Christoffersen et al., 2016

Table S2. Description of simulation treatments of hypothetical droughts from a 'baseline' case (i.e., no drought treatment) to unprecedented climate extremes (UCEs). Varying drought intensity (precipitation removal) from 5% to 100% removal, in increments of 5%, over drought durations of either 1, 2, or 4 years in length. To explore climate change response, we repeated the drought treatments and increased temperature only (+2K over ambient), eCO_2 concentration to 600 ppm and 800 ppm, and increased temperature and eCO_2 (+2K 600 ppm; +2K 800 ppm) and compared to the reference simulation.

	Drought Intensity	Drought Duration	Temperature (K)	CO_2 (ppm)
Baseline	0%	0 years	Ambient	Ambient
Drought Only (Reference)	5% - 100%	1 year	----	----
Drought Only (Reference)	5% - 100%	2 years	----	----
Drought Only (Reference)	5% - 100%	4 years	----	----
Drought + Temp.	5% - 100%	1 year	+ 2K	----
Drought + Temp.	5% - 100%	2 years	+ 2K	----
Drought + Temp.	5% - 100%	4 years	+ 2K	----

Drought + CO$_2$	5% - 100%	1 year	----	+ 200 ppm
Drought + CO$_2$	5% - 100%	2 years	----	+ 200 ppm
Drought + CO$_2$	5% - 100%	4 years	----	+ 200 ppm
Drought + CO$_2$	5% - 100%	1 year	----	+ 400 ppm
Drought + CO$_2$	5% - 100%	2 years	----	+ 400 ppm
Drought + CO$_2$	5% - 100%	4 years	----	+ 400 ppm
Drought + Temp. + CO$_2$	5% - 100%	1 year	+ 2K	+ 400 ppm
Drought + Temp. + CO$_2$	5% - 100%	2 years	+ 2K	+ 400 ppm
Drought + Temp. + CO$_2$	5% - 100%	4 years	+ 2K	+ 400 ppm

1618
1619
1620 **Table S3.** Comparison of *in situ* observations and baseline model simulations from ED2 and
1621 LPJ-GUESS for the two example study sites, Palo Verde in Costa Rica (Kalacska et al., 2005;
1622 Xu et al., 2016) and EucFACE in Australia (Medyln et al., 2016; Duursma et al., 2016). Mean
1623 and ± standard deviation.

	Palo Verde Costa Rica	EucFACE Australia
Obs. Biomass (kgC m^{-2})	11.0 (5.2)	12.7 (4.5)
ED2 Biomass (kgC m^{-2})	11.7 (0.3)	5.6 (0.3)
LPJ-GUESS Biomass (kgC m^{-2})	10.4 (0.2)	12.1 (0.2)
Obs. LAI (m^2 m^{-2})	3.8 (1.06)	1.7 (0.6)
ED2 LAI (m^2 m^{-2})	3.3 (0.1)	1.6 (0.2)
LPJ-GUESS LAI (m^2 m^{-2})	4.5 (0.1)	3.2 (1.3)

1624
1625

Deleted: 2

53
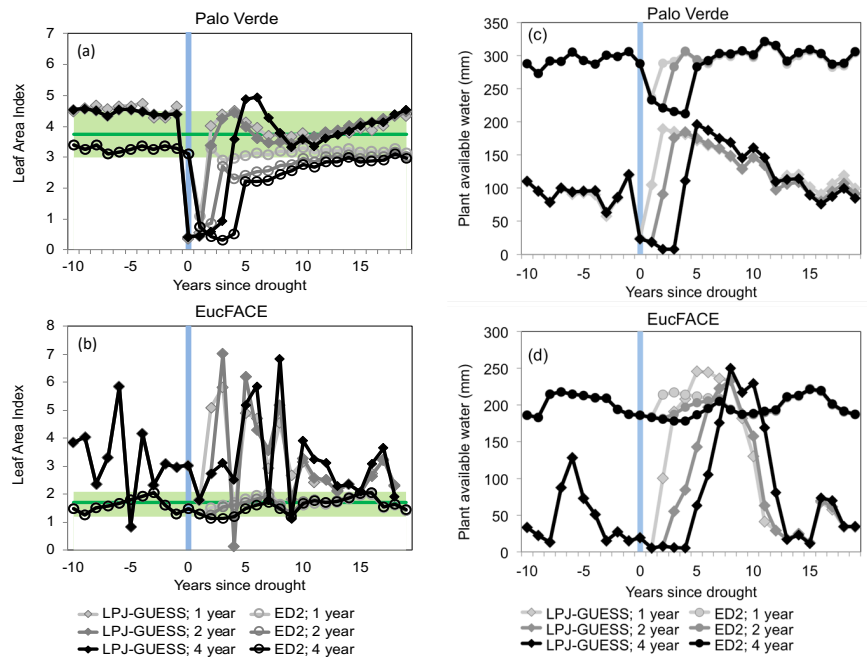
Figure S1. Change in leaf area index (LAI; $m^2 m^2$) (a-b) and annual plant available water (mm) (c-d) as a result of three drought durations events (1 year, 2 year, and 4 year durations) compared to the pre-drought period (i.e. negative years) and over a 20-year recovery period, for both the LPJ-GUESS and ED2 demography models at the Palo Verde site and EucFACE site. Shaded green area is the observed range in LAI from Kalacska et al., (2005) at Palo Verde and Duursma et al., (2016) at EucFACE. The modeled drought intensity at Palo Verde was 90% precipitation removed, and 50% precipitation removed at EucFACE. Plant available water was calculated over a soil depth of 3 meters in ED2 and 2 meters in LPJ-GUESS.
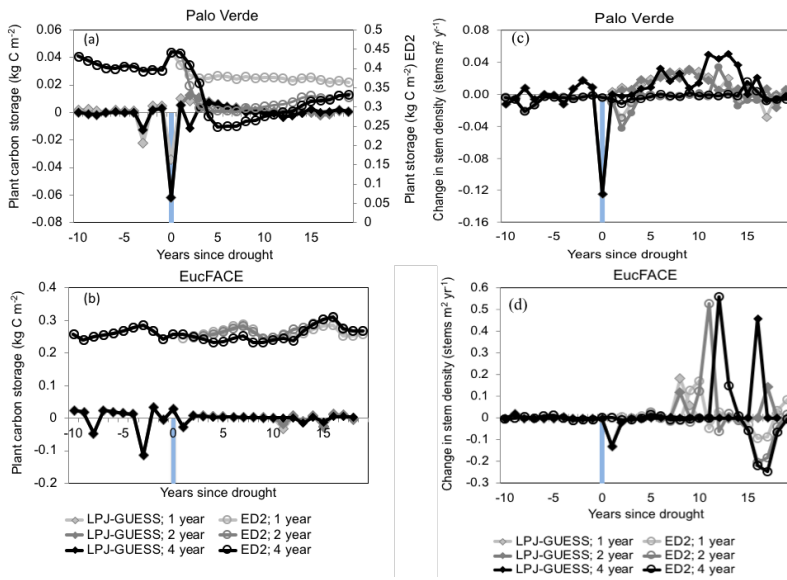
Figure S2. Change in plant carbohydrate storage (kg C m^{-2}) (a-b) and change in stem density (stems m^2 yr^{-1}) (c-d) as a result of three drought durations events (1 year, 2 year, and 4 year durations) compared to the pre-drought period (i.e. negative years) and over a 20-year recovery period, for both the LPJ-GUESS and ED2 demography models at the Palo Verde site and EucFACE site. The modeled drought intensity at Palo Verde was 90% precipitation removed, and 50% precipitation removed at EucFACE.

Supplement Text A:

Site Descriptions:

The Australian EucFACE site has a canopy coverage of 95% (830 trees ha^{-1}) of mature *Eucalyptus* (*E. tereticornis*) evergreen trees. The EucFACE site has a mean annual temperature of 17.3°C, receives an annual rainfall of 800 mm (Ellsworth et al., 2017), with total plant available soil water of 300 mm. The evergreen eucalypt trees are on average 22 m tall with a DBH of 21 cm and a stand-level LAI of 1.7 m^2 m^{-2}. The Costa Rican Palo Verde site has nutrient rich soils (Powers and Peréz-Aviles, 2013), stand basal area is 29.2 (± 8.1) m^2 ha, stem density of 64 (± 12) trees ha^{-1}, and a mean annual temperature of 25.1°C, and mean annual rainfall of 1440 mm, with a 5-month dry season. Multiple leaf phenological strategies co-occur, including evergreens, brevi-deciduous tree species, as well as deciduous species that drop their leaves during the dry season, leading to a strong seasonality in LAI ranging from 3 to 4.5, but can get as low as 1.2 m^2 m^{-2} (Kalacska et al., 2005).

Meteorological data and initial conditions used to drive ED2 and LPJ-GUESS:

Necessary meteorological drivers for ED2 and LPJ-GUESS include incoming radiation (short-wave and long-wave), air temperature, humidity, and pressure, precipitation and wind speed at sub-daily scale. In-situ meteorological data for Palo Verde is only available since 2008. Using the short-term data as the control climate can lead to biases in ecosystem states and high-frequency cyclic ecosystem dynamics before applying UCEs. Therefore, we use re-analysis data (1970 to 2012) at 0.5 degree resolution from Princeton Global Forcing dataset (Sheffield et al., 2006), and was recycled repeatedly for the Palo Verde simulations.

In-situ meteorological data for EucFACE were obtained from a dataset previously compiled for a simulation study of the EucFACE experimental site (Medlyn et al., 2016). Daily time series of air temperature, precipitation, downward shortwave radiation and photosynthetically-active radiation for 1992-2011 were extracted from the 1 × 1° grid cell encapsulating the site from the Princeton Global Forcing data set (Sheffield et al., 2006). This 20-year time series was recycled repeatedly to force the simulations. For both sites, the baseline simulations were initialized as a near-bare-ground situation, with small amount of tree seedlings equally from each PFT. The baseline spin-up lasted for 100 years (ED2) or 780 years (LPJ-GUESS) using recycling natural climate variability as described above.

Review of Model Parameter Uncertainty:

As stated in the manuscript, a goal of this paper is to demonstrate how to use the two VDMs (ED2 and LPJ-GUESS) in order to help generate and test future hypotheses about UCEs. Therefore, we used the models and sites as conceptual "experimental" tools to investigate the given hypotheses and provide a road map for utilizing VDMs. Investigating parameter uncertainty and sensitivity was out of scope for this manuscript. These models are well documented and investigated VDMs, with many previous studies that have looked into parameter uncertainty. Below are a handful of select references (and quick summaries) that explore parameter sensitivities and model uncertainty (in addition to the main manuscripts that

tested the two VDMs at the Palo Verde and EucFACE sites (Xu et al., 2016; Medlyn et al., 2016; Medvigy et al., 2019).

- LPJ-GUESS: "Projected forest carbon fluxes (for European forests) are most sensitive to photosynthesis-, water-, and mortality-related parameters, while predictive uncertainties are dominantly induced by environmental drivers and parameters related to water and mortality." (Oberpriller et al., 2022)
- LPJ-GUESS: "The intrinsic quantum efficiency of CO_2 uptake (*alpha_C3*) and the photosynthesis scaling parameter (from leaf to canopy) (*alpha_a*) as the main contributors of sensitivity for net primary production (NPP) (about 50 %–60 % of the overall sensitivity, Zaehle et al., 2005; Pappas et al., 2013)."
- LPJ-GUESS: The foliage projective cover parameter is sensitivity for net primary production (NPP) (Jiang et al., 2012).
- ED2: After evaluating long-term successional dynamics for a North American Upper Midwest forest authors found that "two parameters related to plant–soil water conductance and growth respiration contributed most to uncertainty in predicted NPP, with both being unobservable empirical coefficients". And "conclude that parameter uncertainty is more important than structural uncertainty, at least for ED-2.2" (Shiklomanov et al., 2020).
- ED2: See Viskari et al., (2019) for a review on the influence of specifically canopy radiation parameter uncertainty in ED2.

Supplement Text B:

Additional knowledge gaps

With so many compounding interactions contributing to ecosystem resistance, impact, and recovery from droughts, there are still knowledge gaps in compounding processes like response to concurrent or repeated extremes, lag affects, or cascades. However, it is difficult for planned experiments to include multiple stressors and very extreme environmental conditions, thus making it challenging to assess all impacts and whether biological ecosystem components (e.g. plant-soil, plant-atmosphere, C:N, respiration-photosynthesis) will remain coupled under extreme conditions. Unfortunately, there is a lack of data on key characteristics and responses to UCEs, which greatly impacts our understanding and ability to predict ecosystem responses to such events. In addition to the general understanding of ecosystem responses to UCEs, we describe some issues which can lead to compounded and notable responses to UCEs.

Concurrent or repeated extremes: As the frequency of extreme climatic events increases, so does the likelihood of experiencing concurrent/combined or repeated extreme events. Combined drought extremes and heat resulted in amplified impacts in the model applications in this study supported by studies showing stronger impact of combined drought-heat extremes on leaf mortality and plant senescence (Dressen et al., 2014). However, the sensitivity of ecosystems to repeated or combined extremes as well as their ability to acclimate remains generally unclear.

Lag effects: Ecosystems must re-establish resilience following an extreme event, but the time needed for a system to do so is difficult to predict due to unanticipated lag effects of extreme events on ecosystem functioning. Previous drought exposure has been linked to long-term mortality of forest trees in the eastern US (Berdanier and Clark, 2016) and to decreased short-term leaf survival in response to additional extreme events (Dreesen et al., 2014) suggesting a time period following disturbance where forests are particularly susceptible to additional stressors. Also, transgenerational effects of drought on leaf stoichiometry (C:N) with direct consequences for ecosystem-level C storage has been detected in perennial plant seedlings (Walter et al., 2016). However, such lag effects are generally difficult to study and are therefore generally poorly understood.

Cascades: Despite our understanding that feedbacks among ecosystem components are likely to impact environmental functioning along multiple pathways and ultimately the terrestrial carbon cycle (Reichstein et al., 2013), empirical studies of cascades are rare (but see Jentsch et al., 2011 for plant-soil measurements). In particular, our ability to predict response thresholds is poor, and additional uncertainty in predicting ecosystem responses occurs because thresholds can be passed at any organizational level within an organism (e.g. leaf, individual, plant community levels; Frank et al., 2015; Gutschick and BassiriRad, 2003) and among organisms (e.g. different sensitivities of soil fungi vs. bacteria to different disturbances; Muhr et al., 2009).

Secondary disturbance: The combination of extreme events and secondary disturbances may increase the susceptibility of carbon loss from ecosystems (e.g., Hicke et al., 2016). For example, extreme droughts and heatwaves promote forest fires by increasing both fuel flammability and lightning strike frequency (Wendler et al., 2011). Substantial forest damage can also occur through phenological changes of forest vegetation or biotic pests or pathogens. Warm winters can weaken wintertime pest mortality and increase pest growth rates (Bale et al., 2002; Cornelissen, 2011), shifting insect phenologies and triggering outbreaks. Water-stressed trees are susceptible to foliar and woody damage from forest insect and pathogens (Jactel et al., 2012, Flowers and Gonzalez-Meler, 2015; Kolb et al., 2016), and combined drought-stress and insect outbreaks can cause massive forest die-off (Allen et al., 2010; Anderegg et al., 2015b) leading to unprecedented levels of tree mortality such as those recorded in western North America (Breshears et al., 2005; Raffa, 2008). Warm winters may advance the leaf-out of deciduous species (Parmesan and Yohe, 2003), increasing their susceptibility to secondary disturbances, such as frost-damage (Gu et al., 2011; Polgar and Primack, 2011). Studies have directly linked such coupled disturbances to a decrease in seasonal C accumulation and to shifts in the development of reproductive structures (Augspurger, 2009), but the global consequences of such phenological shifts and coupled-disturbances has not been quantified (?).

Thresholds: Large-scale ecosystem studies are costly and so rarely include gradients or multiple treatment levels (but see Kreyling et al., 2014). Therefore, our ability to detect and understand tipping points is still very limited. Models could play a significant role in identifying 'zones of sensitivity' that can be targeted in field experiments.

References:

Augspurger, C. K.: Spring 2007 warmth and frost: phenology, damage and refoliation in a temperate deciduous forest, Func, Ecol., 23: 1031–1039. doi:10.1111/j.1365-2435.2009.01587.x, 2009.

Bale, J. S., Masters, G. J., Hodkinson, I. D., Awmack, C., Bezemer, T. M., Brown, V. K., Butterfield, J., Buse, A., Coulson, J. C., Farrar, J., Good, J. E. G., Harrington, R., Hartley, S., Jones, T. H., Lindroth, R. L., Press, M. C., Symrnioudis, I., Watt, A. D. and Whittaker, J. B.: Herbivory in global climate change research: direct effects of rising temperature on insect herbivores, Glob. Change Biol., 8: 1–16. doi:10.1046/j.1365-2486.2002.00451.x, 2002.

Berdanier, A. B. and Clark, J. S.: Multiyear drought-induced morbidity preceding tree death in southeastern U.S. forests, Ecol Appl, 26: 17–23. doi:10.1890/15-0274, 2016.

Breshears, D. D., Cobb, N. S., Rich, P. M., Price, K. P., Allen, C. D., Randy G. Balice, Romme, WH, Kastens, JH, Floyd, M L, Belnap, J, Anderson, JJ, Myers, OB, and Meyer, CW.: Regional Vegetation Die-off in Response to Global-Change-Type Drought, PNAS, 102, 15144–15148, 2005.

Christoffersen, B.O., Gloor, M., Fauset, S., Fyllas, N.M., Galbraith, D.R., Baker, T.R. et al.: Linking hydraulic traits to tropical forest function in a size-structured and trait-driven model (TFS v.1-Hydro), Geosci. Model Dev. Discuss., 2016, 1-60, 2016.

Cornelissen, T.: Climate change and its effects on terrestrial insects and herbivory patterns. Neotrop. entomol. 40, 155-163, http://dx.doi.org/10.1590/S1519-566X2011000200001, 2011.

Druel, A., Ciais, P., Krinner, G., and Peylin, P.: Modeling the vegetation dynamics of northern shrubs and mosses in the ORCHIDEE land surface model, JAMES, 11, 2020– 2035, https://doi.org/10.1029/2018MS001531, 2019.

Duursma, R.A., Gimeno, T.E., Boer, M.M., Crous, K.Y., Tjoelker, M.G. and Ellsworth, D.S.: Canopy leaf area of a mature evergreen *Eucalyptus* woodland does not respond to elevated atmospheric [CO_2] but tracks water availability. Glob. Change Biol., 22, 1666-1676. https://doi.org/10.1111/gcb.13151, 2016.

Eller, C.B., Rowland, L., Mencuccini, M., Rosas, T., Williams, K., Harper, A. et al.: Stomatal optimization based on xylem hydraulics (SOX) improves land surface model simulation of vegetation responses to climate, New Phytol, 226, 1622-1637, https://doi.org/10.1111/nph.16419, 2020.

Fang, Y., Leung, L. R., Knox, R., Koven, C., and Bond-Lamberty, B.: Impact of the numerical solution approach of a plant hydrodynamic model (v0.1) on vegetation dynamics, Geosci. Model Dev., 15, 6385–6398, https://doi.org/10.5194/gmd-15-6385-2022, 2022.

Fisher, R.A., Muszala, S., Verteinstein, M., Lawrence, P., Xu, C., McDowell, N.G. et al.: Taking off the training wheels: the properties of a dynamic vegetation model without climate envelopes, CLM4.5(ED), Geosci. Model Dev., 8, 3593-3619, 2015.

Flowers C.E. and M.A. Gonzalez-Meler: Responses of temperate forest productivity to insect and pathogen disturbances, Ann Rev Plant Sci, 66:547-569, 2015.

Frank, D., Reichstein, M., Bahn, M., Thonicke, K., Frank, D., Mahecha, M. D., Smith, P., van der Velde, M., Vicca, S., Babst, F., Beer, C., Buchmann, N., Canadell, J. G., Ciais, P., Cramer, W., Ibrom, A., Miglietta, F., Poulter, B., Rammig, A., Seneviratne, S. I., Walz, A.,

1834   Wattenbach, M., Zavala, M. A. and Zscheischler, J.: Effects of climate extremes on the
1835   terrestrial carbon cycle: concepts, processes and potential future impacts, Glob. Change
1836   Biol., 21, 2861–2880, doi:10.1111/gcb.12916, 2015.
1837 Gutschick, V. P. and BassiriRad, H.: Extreme events as shaping physiology, ecology, and
1838   evolution of plants: toward a unified definition and evaluation of their consequences, New
1839   Phytol., 160, 21–42, doi:10.1046/j.1469-8137.2003.00866.x, 2003.
1840 Haverd, V., Smith, B., Nieradzik, L., Briggs, P. R., Woodgate, W., Trudinger, C. M., Canadell, J.
1841   G., and Cuntz, M.: A new version of the CABLE land surface model (Subversion revision
1842   r4601) incorporating land use and land cover change, woody vegetation demography, and a
1843   novel optimisation-based approach to plant coordination of photosynthesis, Geosci. Model
1844   Dev., 11, 2995–3026, https://doi.org/10.5194/gmd-11-2995-2018, 2018.
1845 Hicke, J.A., A.J.H. Meddens, C.A. Kolden: Recent tree mortality in the western United States
1846   from bark beetles and forest fires, Forest Science 62, 141-153, 2016.
1847 Jactel, H., Petit, J., Desprez-Loustau, M.-L., Delzon, S., Piou, D., Battisti, A. and Koricheva, J.:
1848   Drought effects on damage by forest insects and pathogens: a meta-analysis, Glob. Change
1849   Biol., 18, 267–276. doi:10.1111/j.1365-2486.2011.02512.x, 2012.
1850 Jentsch, A., Kreyling, J., Elmer, M., Gellesch, E., Glaser, B., Grant, K., et al.: Climate extremes
1851   initiate ecosystem-regulating functions while maintaining productivity, J. of Ecol., 99, 689–
1852   702, doi:10.1111/j.1365-2745.2011.01817.x, 2011.
1853 Jiang, Y., Zhuang, Q., Schaphoff, S., Sitch, S., Sokolov, A., Kicklighter, D., and Melillo, J.:
1854   Uncertainty analysis of vegetation distribution in the northern high latitudes during the 21st
1855   century with a dynamic vegetation model, Ecol. Evol., 2, 593-
1856   614, https://doi.org/10.1002/ece3.85, 2012.
1857 Kalacska, M.E.R., Sánchez-Azofeifa, G.A., Calvo-Alvarado, J.C., Rivard, B. and Quesada, M.:
1858   Effects of Season and Successional Stage on Leaf Area Index and Spectral Vegetation
1859   Indices in Three Mesoamerican Tropical Dry Forests. Biotropica, 37: 486-
1860   496. https://doi.org/10.1111/j.1744-7429.2005.00067.x, 2005.
1861 Krinner, G., N. Viovy, N. de Noblet-Ducoudré, J. Ogée, J. Polcher, P. Friedlingstein, P. Ciais, S.
1862   Sitch, and I. C. Prentice: A dynamic global vegetation model for studies of the coupled
1863   atmosphere-biosphere system, Glob. Biogeochemical Cycles, 19, GB1015,
1864   doi:10.1029/2003GB002199, 2005.
1865 Lawrence, D. M., Fisher, R. A., Koven, C. D., Oleson, K. W., Swenson, S. C., Bonan, G., et
1866   al.: The Community Land Model version 5: Description of new features, benchmarking, and
1867   impact of forcing
1868   uncertainty, JAMES, 11, 4245– 4287, https://doi.org/10.1029/2018MS001583, 2019.
1869 Li, L., Yang, Z.-L., Matheny, A. M., Zheng, H., Swenson, S. C., Lawrence, D. M., et
1870   al.: Representation of plant hydraulics in the Noah-MP land surface model: Model
1871   development and multiscale evaluation, JAMES, 13,
1872   e2020MS002214, https://doi.org/10.1029/2020MS002214, 2021.
1873 Medlyn, B.E., De Kauwe, M.G., Zaehle, S., Walker, A.P., Duursma, R.A., Luus, K., Mishurov,
1874   M., Pak, B., Smith, B., Wang, Y.-P., Yang, X., Crous, K.Y., Drake, J.E., Gimeno, T.E.,
1875   Macdonald, C.A., Norby, R.J., Power, S.A., Tjoelker, M.G., and Ellsworth, D.S.: Using
1876   models to guide field experiments: a priori predictions for the CO2 response of a nutrient-
1877   and water-limited native Eucalypt woodland, Glob. Change Biol., 22, 2834-2851, 2016.

Muhr, J., Borken, W. and Matzner, E.: Effects of soil frost on soil respiration and its radiocarbon
   signature in a Norway spruce forest soil, Glob. Change Biol., 15, 782–793,
   doi:10.1111/j.1365-2486.2008.01695.x, 2009.
Nabel, J. E. M. S., Naudts, K., and Pongratz, J.: Accounting for forest age in the tile-based
   dynamic global vegetation model JSBACH4 (4.20p7; git feature/forests) – a land surface
   model for the ICON-ESM, Geosci. Model Dev., 13, 185–200, https://doi.org/10.5194/gmd-
   13-185-2020, 2020.
Oberpriller, J., Herschlein, C., Anthoni, P., Arneth, A., Krause, A., Rammig, A., Lindeskog, M.,
   Olin, S., and Hartig, F.: Climate and parameter sensitivity and induced uncertainties in
   carbon stock projections for European forests (using LPJ-GUESS 4.0), Geosci. Model Dev.,
   15, 6495–6519, https://doi.org/10.5194/gmd-15-6495-2022, 2022.
Pappas, C., Fatichi, S., Leuzinger, S., Wolf, A., and Burlando, P.: Sensitivity analysis of a
   process-based ecosystem model: Pinpointing parameterization and structural issues, J.
   Geophys. Res.-Biogeo., 118, 505–528, https://doi.org/10.1002/jgrg.20035, 2013.
Parmesan, C and G. Yohe: A globally coherent fingerprint of climate change impacts across
   natural systems, Nature, 421, 37-42, 2003.
Polgar, C. A. and Primack, R. B.: Leaf-out phenology of temperate woody plants: from trees to
   ecosystems, New Phytol., 191, 926–941, doi:10.1111/j.1469-8137.2011.03803.x, 2011.
Raffa, K. F.: Cross-scale drivers of natural disturbances prone to anthropogenic amplification: the
   dynamics of bark beetle eruptions, BioScience, 58, 501-517, 2008.
Reichstein, M, Bahn, M, Ciais, P, Frank, D, Mahecha, MD, Seneviratne, SI, Zscheischler, J, Beer,
   C, Buchmann, N, Frank, DC, Papale, D, Rammig, A, Smith, P, Thonicke, K, van der Velde,
   M, Vicca, S, Walz, A and Wattenbach, M.: Climate extremes and the carbon cycle, Nature,
   500, 287-295, 2013.
Sato, H., Itoh, A., and Kohyama, T.: SEIB–DGVM: A new Dynamic Global Vegetation Model
   using a spatially explicit individual-based approach, Ecol.
   Model., 200, 279– 307. https://doi.org/10.1016/j.ecolmodel.2006.09.006, 2007.
Sheffield, J., Goteti, G., and Wood, E.F.: Development of a 50-year high-resolution global dataset
   of meteorological forcings for land surface modeling, J. Clim., 19, 3088–3111, 2006.
Shiklomanov, AN, Bond-Lamberty, B, Atkins, JW, Gough, CM.: Structure and parameter
   uncertainty in centennial projections of forest community structure and carbon
   cycling, Glob. Change Biol., 26, 6080– 6096, https://doi.org/10.1111/gcb.15164, 2020.
Smith, B., Prentice, I.C., and Sykes, M.T.: Representation of vegetation dynamics in the
   modelling of terrestrial ecosystems: comparing two contrasting approaches within European
   climate space, Global Ecol. Biogeo., 10, 621-637, 2001.
Smith, B., Wårlind, D., Arneth, A., Hickler, T., Leadley, P., Siltberg, J. et al.: Implications of
   incorporating N cycling and N limitations on primary production in an individual-based
   dynamic vegetation model, Biogeosciences, 11, 2027-2054, 2014.
Viskari T., Shiklomanov A., Dietze M.C., Serbin S.P.: The influence of canopy radiation
   parameter uncertainty on model projections of terrestrial carbon and energy cycling, PLoS
   ONE 14, e0216512, https://doi.org/10.1371/journal.pone.0216512, 2019.
Walter, J., Harter, D. E. V., Beierkuhnlein, C. and Jentsch, A.: Transgenerational effects of
   extreme weather: perennial plant offspring show modified germination, growth and
   stoichiometry, J Ecol, doi:10.1111/1365-2745.12567, 2016.
Wang, Y. P., Kowalczyk, E., Leuning, R., Abramowitz, G., Raupach, M. R., Pak, B., et
   al.: Diagnosing errors in a land surface model (CABLE) in the time and frequency

domains. J. of Geo. Res.:
Biogeosciences, 116, 1– 18, https://doi.org/10.1029/2010JG001385, 2011.

Weng, E.S., Malyshev, S., Lichstein, J.W., Farrior, C.E., Dybzinski, R., Zhang, T. et al.: Scaling
from individual trees to forests in an Earth system modeling framework using a
mathematically tractable model of height-structured competition, Biogeosciences, 12, 2655-
2694, 2015.

Wendler G, Conner J, Moor B, Shulski M, Stuefer M.: Climatology of Alaskan wildfires with
special emphasis on the extreme year of 2004, Theoretical and Applied Climatology, 104,
459–472, 2011.

Xu, X., Medvigy, D., Powers, J.S., Becknell, J.M. and Guan, K.: Diversity in plant hydraulic
traits explains seasonal and inter-annual variations of vegetation dynamics in seasonally dry
tropical forests, New Phytol., 212, 80-95, 2016.

Xu, X., Konings, A.G., Longo, M., Feldman, A., Xu, L., Saatchi, S., Wu, D., Wu, J. and
Moorcroft, P.: Leaf surface water, not plant water stress, drives diurnal variation in tropical
forest canopy water content, New Phytol, 231, 122-136, https://doi.org/10.1111/nph.17254,
2021.

Zaehle, S., Sitch, S., Smith, B., and Hatterman, F.: Effects of parameter uncertainties on the
modeling of terrestrial biosphere dynamics, Global Biogeochem. Cy., 19,
GB3020, https://doi.org/10.1029/2004GB002395, 2005.